Informes Técnicos Ciemat **1081**
Julio, 2006

# Behaviour of MX-80 Bentonite at Unsaturated Conditions and under Thermo-Hydraulic Gradient

M.V. Villar
R. Gómez-Espina
P.L. Martín

**Departamento de Medio Ambiente**

**Behaviour of MX-80 Bentonite at Unsaturated Conditions and under Thermo-Hydraulic Gradient**
**- Work Performed by CIEMAT in the Context of the TBT Project -**

Villar, M.V.; Gómez-Espina, R.; Martín, P.L.

51 pp. 52 figs. 9 refs.

**Abstract:**
This document reports the thermo-hydro-mechanical characterisation of the MX-80 bentonite performed at CIEMAT between 2004 and 2006 in the context of the Agreement CIEMAT/CIMNE 04/113. This Agreement took place in the framework of the Temperature Buffer Test (TBT) Project, Whose experimental part is going on at the undergroun research laboratory of Äspö (Sweden) and in which the MX-80 bentonite is used as sealing material in a large scale test. A methodology has been developed for the determination of retention curves at high temperature, what has allowed checking the decrease of the retention capacity of the bentonite with temperature. Infiltration and infiltration/heating tests have been carried out, some of them with simultaneous measurement of temperature and relative humidity.

**Comportamiento de la Bentonita MX-80 en Condiciones no Saturadas y bajo Gradiente Termohidraúlico**
**- Trabajo Realizado en CIEMAT en el Contexto del Proyecto TBT -**

Villar, M.V.; Gómez-Espina, R.; Martín, P.L.

51 pp. 52 figs. 9 refs.

**Resumen:**
Este documento detalla los resultados de la caracterización termo-hidro-mecánica (THM) de la bentonita MX-80 realizada en CIEMAT entre los años 2004 y 2006 en el contexto del Acuerdo CIEMAT/CIMNE 04/113. Este Acuerdo se enmarca en el proyecto Temperature Buffer Test (TBT), cuya parte experimental se lleva a cabo en el laboratorio subterráneo de Äspo (Suecia) y en el que se utiliza bentonita MX-80 como material de sellado en un ensayo a gran escala. Se ha determinado la influencia de la temperatura en la capacidad de retención de la bentonita, para lo quñe se ha desarrollado una metodología específica que ha permitido comprobar la disminución de la capacidad de retención con la temperatura. Se han realizado ensayos de infiltración y de infiltración y calentamiento simultáneos, algunos de ellos con medida simultánea de la temperatura y la humedad relativa en la bentonita.

CLASIFICACIÓN DOE Y DESCRIPTORES

S11
HIGH-LEVEL RADIOACTIVE WASTES; THERMODYNAMIC PROPERTIES; MECHANICAL PROPERTIES; CLAYS; GEOCHEMISTRY; RADIOACTIVE WASTE STORAGE; MATHEMATICAL MODELS; COMPUTER CODES; CHEMICAL PROPERTIES; BENTONITE; RADIOACTIVE WASTE STORAGE

# BEHAVIOUR OF MX-80 BENTONITE AT UNSATURATED CONDITIONS AND UNDER THERMO-HYDRAULIC GRADIENT

WORK PERFORMED BY CIEMAT IN THE CONTEXT OF THE TBT PROJECT

## Table of contents

# 1. INTRODUCTION

This report details the results of the thermo-hydro-mechanical (THM) characterisation of the MX-80 bentonite carried out by CIEMAT (Soil Mechanics Laboratory) from 2004 to 2006 in the context of an agreement between CIEMAT and CIMNE (Centro Internacional de Métodos Numéricos en Ingeniería, Barcelona) to study the behaviour of the MX-80 bentonite in unsaturated conditions and under thermo-hydraulic gradient (Agreement CIEMAT/CIMNE 04/113). The agreement took place in the context of the participation of CIMNE and ENRESA in the project Temperature Buffer Test (TBT), performed by ANDRA and SKB at the Äspö Hard Rock Laboratory (Sweden). The participation of CIEMAT has consisted on the performance of laboratory tests to support the THM modelling work carried out by CIMNE.

The TBT project is a full-scale test for high-level radioactive waste disposal that aims at improving the current understanding of the THM behaviour of buffers with a temperature around and above 100°C during the water saturation transient. The French organisation ANDRA is running this test in cooperation with SKB (Svensk Kärnbränslehantering AB 2005). Two electrical heaters simulating the waste containers were placed in an 8-m depth and 1.8-m diameter vertical hole drilled in granitic rock (Figure 1). The dimensions of the heaters are 3 m in length and 0.6 m in diameter. The lower heater is surrounded by annular blocks of MX-80 bentonite of thickness 0.55 m. The upper heater has a ring of sand between it and the bentonite buffer as a thermal protection to reduce the temperature in the bentonite. The sand ring is 0.20-m thick and the compacted annular blocks of MX-80 have a thickness of 0.35 m. The bentonite has been compacted at dry densities of 1.69 and 1.79 g/cm$^3$, previously adding water to the bentonite so that to obtain a water content of 17.5 percent (Hökmark & Fälth 2003). In this way the initial degree of saturation of the barrier is very high.

The operation phase, including heating, artificial pressurised saturation of the buffer and monitoring of temperature, humidity, pressure and displacement started in March 2003, with an expected duration time of 32 months. Monitoring and sampling of experimental data are continuously ongoing. The dense arrays of thermocouples enable the evaluation of thermal conductivity distribution, which in turn give an indication of the saturation process.

The principle of the TBT test is to observe, understand and model the behaviour of the components in the deposition hole, starting from an initial unsaturated state under thermal transient and ending with a final saturated state with a stable heat gradient. Heat transfer comes into play from the start of the test, possibly redistributing water being present in the buffers, with partial desaturation of very hot zones (> 100°C). In addition, inflow of water causes saturation and consequent swelling of the bentonite.

CIMNE, as a subcontractor to ENRESA, is performing part of the THM modelling of the clay barrier behaviour. To support this modelling work, and specifically to improve the knowledge of the THM behaviour of the clay, CIEMAT has carried out the following laboratory work, which was suggested by the modelling team:

- Determination of the water retention curves of compacted MX-80 bentonite at high temperatures.

- Design, manufacturing and launching of infiltration tests, with study of the bentonite once the experiments finished.

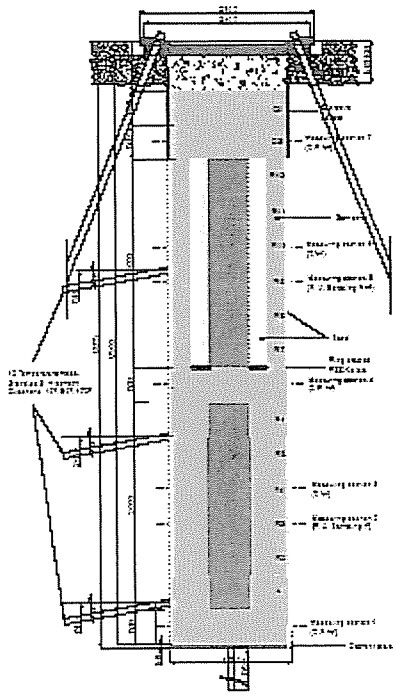

Figure 1: Experimental setup of the TBT experiment (Svensk Kärnbränslehantering AB 2005)

## 2. MATERIAL

The MX-80 clay is extracted from Wyoming (USA), and has been selected in many disposal concepts as backfilling and sealing material (Sweden, Finland, Germany, France). It is a worldwide known material supplied in the form of powder homoionised to sodium (SKB reports, Müller-Vonmoss & Kahr 1983, Madsen 1998). The MX-80 bentonite is composed mainly by montmorillonite (65-82%) and it also contains quartz (4-12%), feldspars (5-8%), and smaller quantities of cristobalite, calcite and pyrite. The less than 2 μm fraction of this bentonite is 80-90% of the total. The CEC is 74 meq/100g, and the major exchangeable cations are: Na (61 meq/100g), Ca (10 meq/100g) and Mg (3 meq/100g). The liquid limit of the bentonite is 350-570 percent, the plastic limit 70 percent and the specific weight of the solid particles –determined with pycnometers using deionised water as suspension medium– is 2.82.

The swelling pressure of the bentonite compacted at dry density 1.60 g/cm$^3$ is about 7.5 MPa and the hydraulic conductivity for the same dry density is in the order of $10^{-13}$ m/s (Villar 2005).

The MX-80 clay used in the tests performed by CIEMAT is a 10-kg batch provided in November 2004 by Clay Technology AB. Its hygroscopic water content under the CIEMAT laboratories conditions is around 11 percent. The liquid limit is 526 percent and the plastic limit is 46 percent, resulting in a plasticity index of 480. The BET specific surface area is 16 m$^2$/g. Some of the tests performed at the beginning of this research were done with bentonite from a different batch, sent to CIEMAT in April 1996. The hygroscopic water content of the

bentonite from this first batch at laboratory conditions is 9 percent. The lower hygroscopic water content reflects probably the lower purity of the first batch.

## 3. RETENTION CURVES

### 3.1 Methodology

A methodology has been developed to determine in an easy way the retention curves of the compacted bentonite at different temperatures. It consists on the measurement of the relative humidity of a bentonite block by means of a capacitive sensor. The block is kept inside a cylindrical hermetic cell made out of stainless steel (Figure 2). After mixing the clay with the appropriated water quantity, the bentonite is compacted to the desired dry density and the resulting block is introduced in the cell, the dimensions of the block being equal to the internal volume of the cell, 7 cm diameter and 10 cm height. A hole is drilled in the central, upper part of the block to insert the sensor and the cell is closed. The upper lid of the cell has a central perforation to allow the passage of the sensor cable.

The transmitters used are VAISALA HMP237 or HMP233, that include a humidity sensor which changes its electrical characteristics with extremely small variations in humidity (capacitive type relative humidity sensor). They include also a temperature sensing system (Pt 100). The accuracy of the humidity sensor is ±1 percent over the range 0-90 percent *RH* and ±2 percent over the range 90-100 percent *RH*. To convert the values of relative humidity (*RH*, %) to suction values (*s*, MPa) the Kelvin's law has been used:

$$s = -10^{-6}\frac{R\times T}{V_w}\ln\left(\frac{RH}{100}\right) \qquad [1]$$

where $R$ is the universal constant of gases (8.3143 J/mol·K), $T$ the absolute temperature and $V_w$, the molar volume of water ($1.80\cdot10^{-5}$ $m^3$/mol).

The imperviousness of the cell is guaranteed by using high-temperature resistant sealing adhesive between the cell body and the covers and in the sensor insertion hole. The external wall of the cell is covered with a silicone-rubber laminated heater that fixes the temperature all around the cell. The assembly is wrapped in isolating material. The thermal equilibrium is reached very quickly. After a time long enough to reach a stable measurement of relative humidity, the temperature is changed, what allows, in a single test, the determination of the change of suction with temperature for a given density and water content. Four cells are now in operation (Figure 3).

At the end of the test, the block is extracted (Figure 4), weighed and cut into four vertical sections, and the water content and dry density of each section are measured.

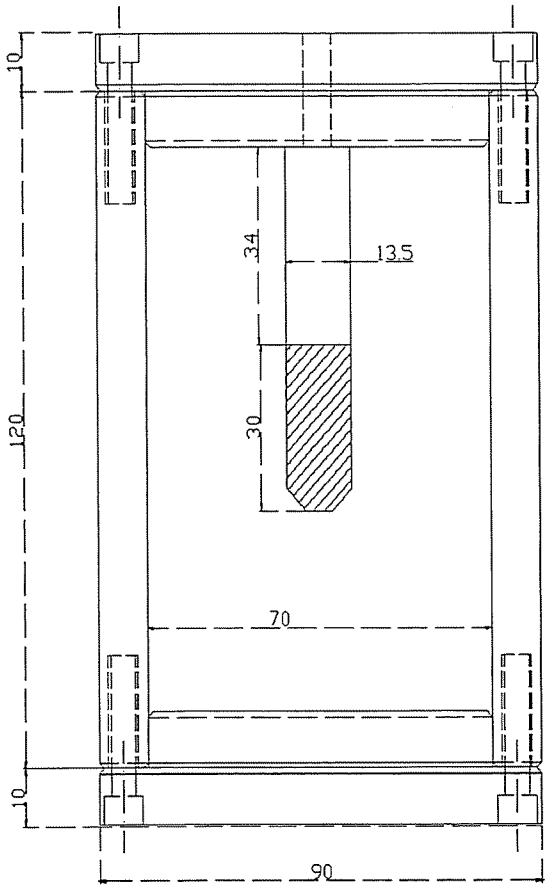


Figure 2. Layout of the cell for the measurement of suction at high temperature with the capacitive sensor inserted in it (dimensions in mm)

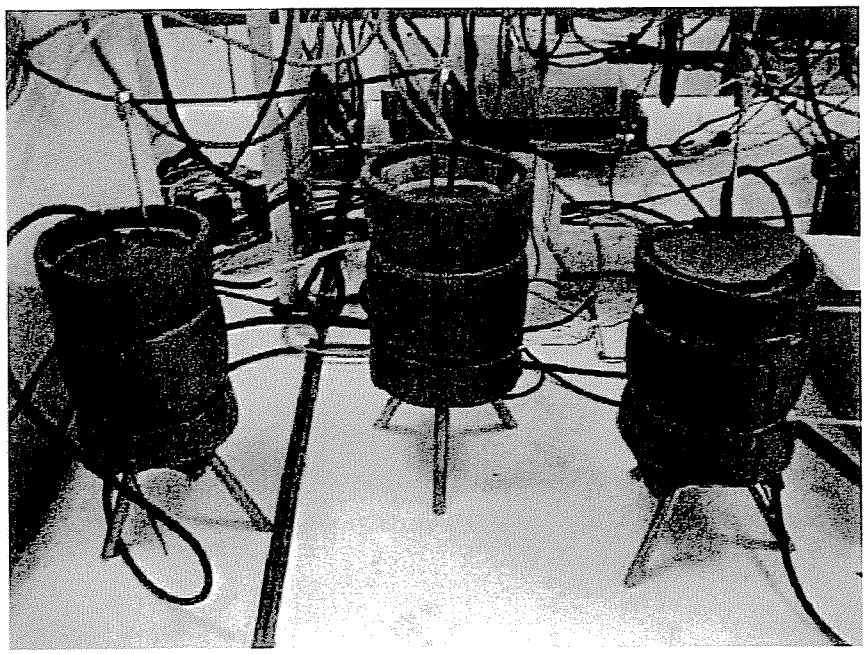

Figure 3: Cells mounted for the determination of retention curves at high temperature, surrounded by an isolating material

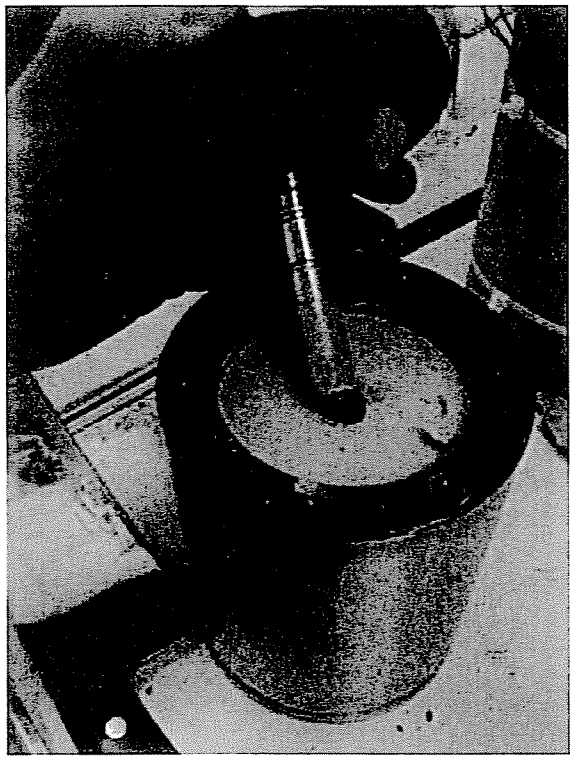

Figure 4: Appearance of the sensor and the bentonite block upon dismantling

### 3.2 Results

The sensor/cell method has been used to measure the change of suction of MX-80 bentonite compacted at nominal dry densities of 1.75 and 1.60 g/cm$^3$ during heating/cooling. The clay was used either with its hygroscopic water content or mixed with deionised water so that to obtain water contents of between 11 and 22 percent. A block was compacted with each water content and placed in the cell. After measuring the suction corresponding to the laboratory temperature, the temperature of the external heating mat was increased up to 100 or 120°C in intervals. Afterwards, the temperature was decreased. The temperature and relative humidity were recorded every 6 hours.

#### 3.2.1 Tests with bentonite compacted at nominal dry density 1.75 g/cm$^3$

Table I summarises the characteristics of the tests carried out with the MX-80 bentonite compacted to nominal dry density 1.75 g/cm$^3$. The initial and final water contents ($w$) and dry densities ($\rho_d$) are indicated. In principle there should not be any difference between the initial and the final values, but in some of the tests the cell lost its imperviousness during heating, and this caused a decrease of the initial water content and an increase of dry density (tests 1.75_15, 1.75_16_2 and 1.75_22). The uniaxial pressure applied to manufacture the blocks is also indicated ($P$).

After measuring the suction corresponding to the laboratory temperature, the temperature of the external heating mat was increased from 30 to 100°C in intervals of 10°C. Each target temperature was kept for about seven days, the suction measured during this period remaining quite constant (Figure 5). Afterwards, temperature was decreased according to the same pattern. The 15-percent water content sample was tested up to 120°C. At this

temperature the cell lost its imperviousness, what gave place to a quick increase of suction (Figure 6), and the test had to be terminated. The same happened in test 1.75_16_2 when the temperature was increased to 125°C and in test 1.75_22 when it was increased to 103°C.

The average equilibrium values of suction measured for each temperature are shown in Table II and plotted in Figure 7. These values are shown in Figure 8 and Figure 9 in the form of retention curves for heating and cooling, respectively. They show a decrease of the retention capacity with temperature, both on heating and on cooling.

At the end of the tests, the water content in different positions inside the bentonite block was checked: it is slightly higher –less than 0.5 percent– in the upper part of the blocks.

Table I: Characteristics of the tests performed with bentonite compacted at nominal $\rho_d$ 1.75 g/cm$^3$

| Reference | Compaction $P$ (MPa) | Initial $w$ (%) | Initial $\rho_d$ (g/cm$^3$) | Final $w$ (%) | Final $\rho_d$ (g/cm$^3$) |
|---|---|---|---|---|---|
| 1.75_9 | 46 | 9.0 | 1.75 | 8.7 | 1.74 |
| 1.75_15 | 62 | 15.0 | 1.79 | 9.6 | 1.85 |
| 1.75_16 | 60 | 16.1 | 1.77 | 15.8 | 1.76 |
| 1.75_16_2 | 50 | 17.6 | 1.73 | 7.1 | 1.84 |
| 1.75_20 | 143 | 18.8 | 1.76 | 18.8 | 1.76 |
| 1.75_22 | | 22.0 | 1.72 | 16.6 | 1.75 |

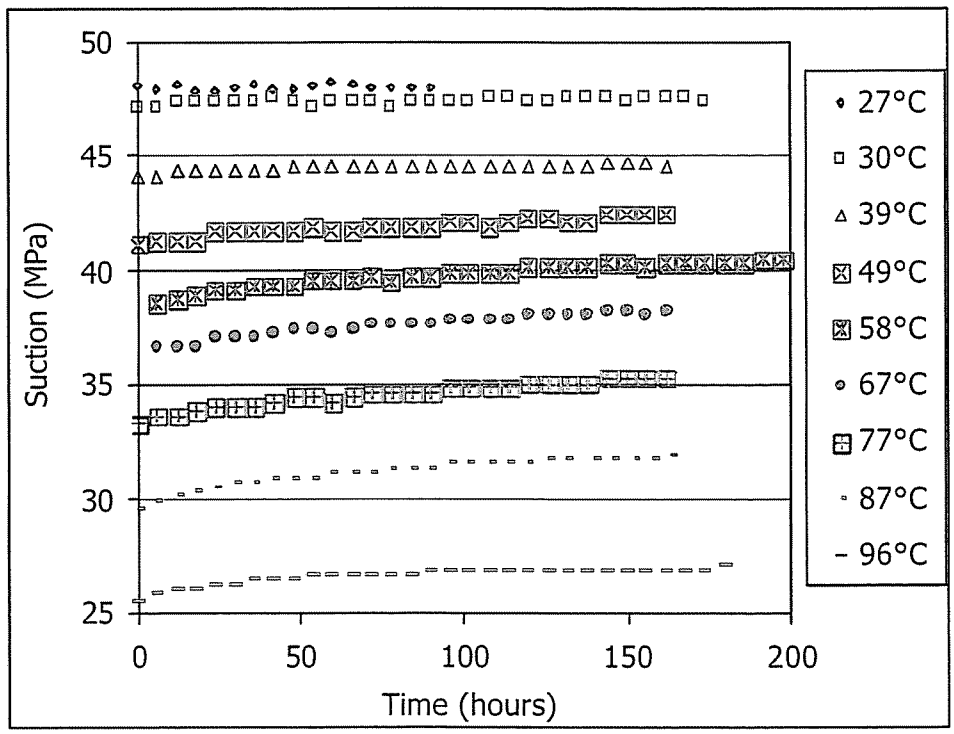


Figure 5: Evolution of suction measured on heating MX-80 bentonite compacted at 1.75 g/cm$^3$ with 16 percent water content (test 1.75_16)

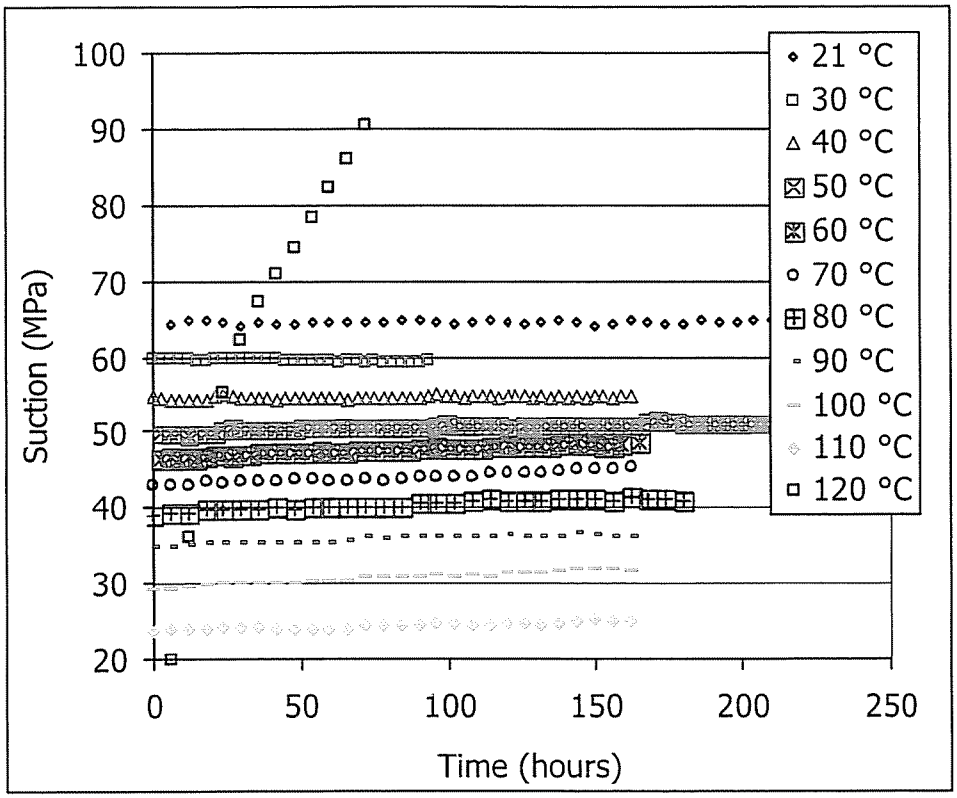


Figure 6: Evolution of suction measured on heating MX-80 bentonite compacted at 1.75 g/cm$^3$ with 15 percent initial water content (test 1.75_15)

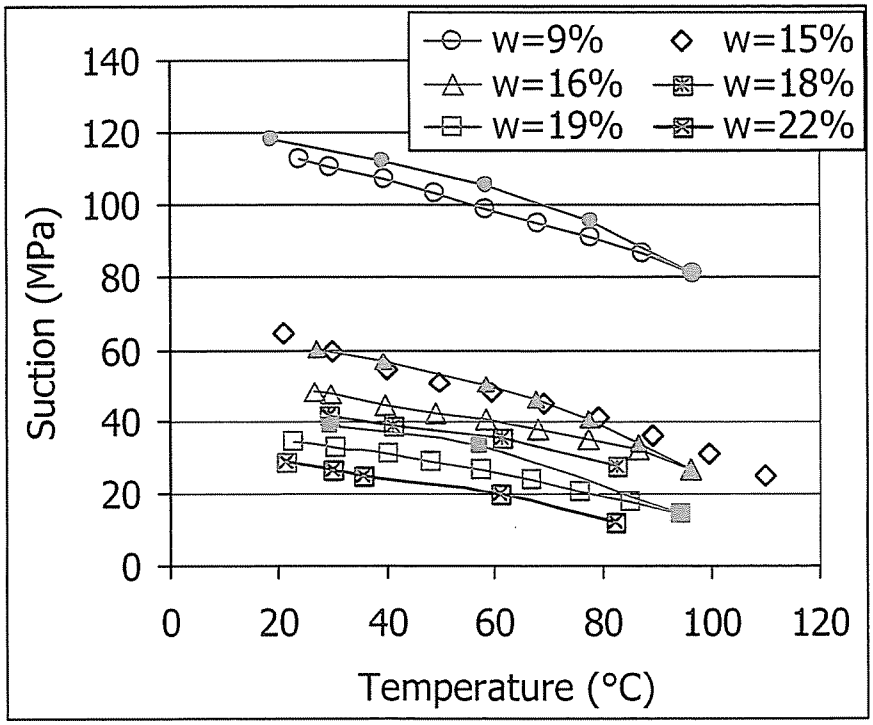


Figure 7: Equilibrium suction measured during heating/cooling in blocks of MX-80 bentonite compacted at 1.75 g/cm$^3$ with different water contents (bold symbols: cooling)

Table II: Equilibrium temperatures and suctions measured during heating/cooling of MX-80 bentonite compacted at nominal $\rho_d$ 1.75 g/cm$^3$ with different water contents (see Table I for acutal values of $\rho_d$ and $w$)

| **1.75_9** | | **1.75_15** | | **1.75_16** | | **1.75_16_2** | | **1.75_20** | | **1.75_22** | |
|---|---|---|---|---|---|---|---|---|---|---|---|
| $T$ (°C) | $s$ (MPa) | $T$ (°C) | $s$ (MPa) | $T$ (°C) | $s$ (MPa) | $T$ (°C) | $s$ (MPa) | $T$ (°C) | $s$ (MPa) | $T$ (°C) | $s$ (MPa) |
| 24 | 113 | 21 | 65 | 27 | 48 | 29 | 41 | 23 | 35 | 22 | 29 |
| 30 | 110 | 30 | 60 | 30 | 47 | 41 | 39 | 31 | 33 | 30 | 26 |
| 39 | 107 | 40 | 55 | 39 | 45 | 61 | 35 | 40 | 31 | 36 | 25 |
| 49 | 103 | 50 | 51 | 49 | 42 | 83 | 28 | 48 | 29 | 61 | 20 |
| 59 | 99 | 60 | 48 | 58 | 40 | 104 | 32 | 58 | 27 | 82 | 12 |
| 68 | 95 | 69 | 45 | 68 | 38 | | | 67 | 24 | | |
| 78 | 91 | 79 | 41 | 77 | 35 | | | 76 | 21 | | |
| 87 | 87 | 89 | 36 | 87 | 32 | | | 85 | 18 | | |
| 97 | 82 | 99 | 31 | 96 | 27 | | | 94 | 15 | | |
| 78 | 96 | 110 | 25 | 87 | 34 | | | 57 | 33 | | |
| 58 | 106 | | | 77 | 40 | | | 30 | 39 | | |
| 39 | 113 | | | 68 | 46 | | | | | | |
| 19 | 118 | | | 58 | 50 | | | | | | |
| | | | | 39 | 57 | | | | | | |
| | | | | 27 | 60 | | | | | | |

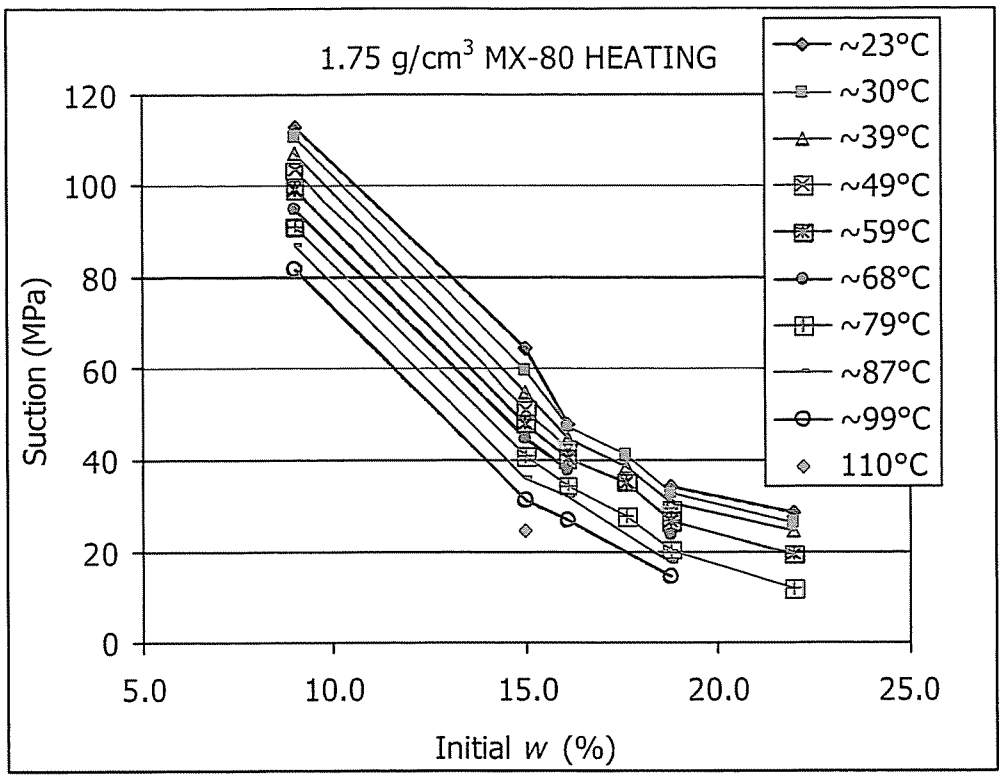


Figure 8: Retention curves obtained during heating with the sensor/cell method for the MX-80 bentonite compacted at 1.75 g/cm$^3$

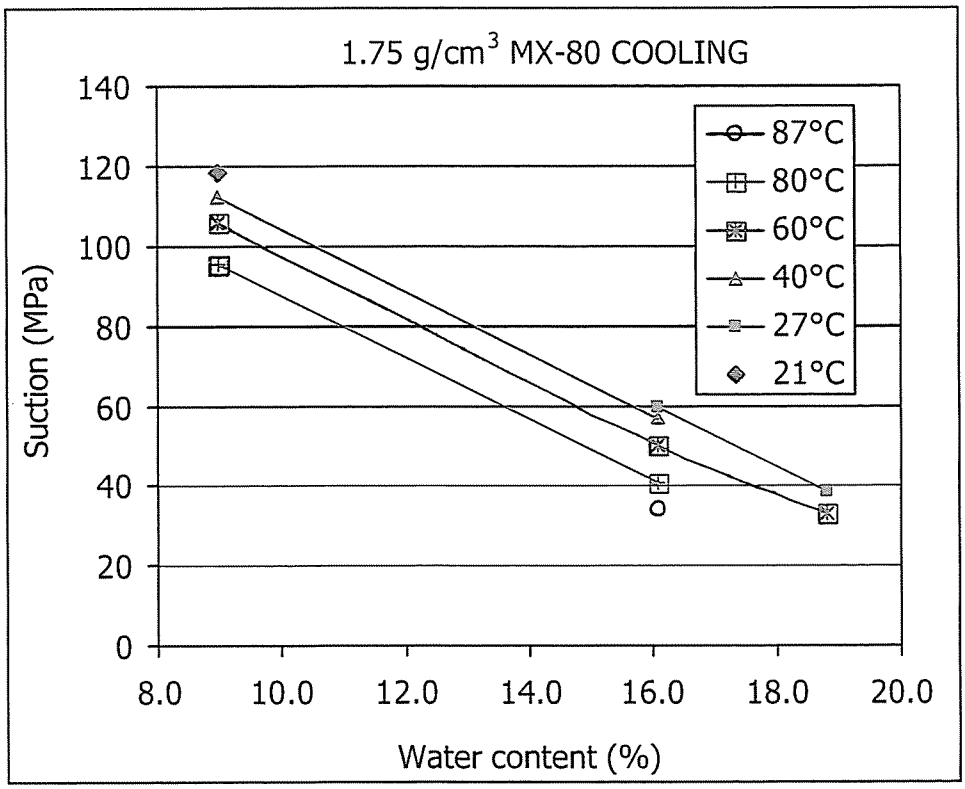


Figure 9: Retention curves obtained during cooling with the sensor/cell method for the MX-80 bentonite compacted at 1.75 g/cm$^3$

### 3.2.2 Tests with bentonite compacted at nominal dry density 1.60 g/cm$^3$

Table III summarises the characteristics of the tests carried out with the MX-80 bentonite compacted to nominal dry density 1.60 g/cm$^3$. The initial and final water contents ($w$) and dry densities ($\rho_d$) are indicated. In principle there should not be any difference between the initial and the final values, but in some of the tests the cell lost its imperviousness during heating, and this caused a decrease of the initial water content and an increase of dry density (tests 1.60_13 and 1.60_19). The uniaxial pressure applied to manufacture the blocks is also indicated ($P$). Sample 1.60_17 was mistakenly compacted to a dry density of 1.66 g/cm$^3$, what clearly affects its hydraulic behaviour. For this reason, the results from this test will not be shown in the figures below.

After measuring the suction corresponding to the laboratory temperature, the temperature of the external heating mat was increased from 40 to 120°C in intervals of 20°C. Each target temperature was kept for about two days. Afterwards, the temperature was decreased according to the same pattern. Figure 10 shows the evolution of suction measured in test 1.60_13 during heating. When the temperature increased from 100 to 120°C the airtightness of the cell was lost and a sharp increase of suction was measured. The same happened in test 1.60_19 when temperature reached 100°C.

The average equilibrium values of suction measured for each temperature are shown in Table IV and plotted in Figure 11. These values are shown in Figure 12 for heating and in Figure 13 for cooling in the form of retention curves. They show a decrease of the retention capacity with temperature, both on heating and on cooling.

At the end of the tests, the water content in different positions inside the bentonite block was checked. The variation among the different samples tested in a block is less than 1 percent, with no clear trend along the height or the radius of the block.

Table III: Characteristics of the tests performed with bentonite compacted at nominal $\rho_d$ 1.60 g/cm$^3$ (except sample 1.60_17)

| Reference | Compaction $P$ (MPa) | Initial $w$ (%) | Initial $\rho_d$ (g/cm$^3$) | Final $w$ (%) | Final $\rho_d$ (g/cm$^3$) |
|---|---|---|---|---|---|
| 1.60_11 | 29 | 10.7 | 1.61 | 11.0 | 1.61 |
| 1.60_13 | | 13.1 | 1.62 | 11.3 | 1.63 |
| 1.60_15 | | 14.9 | 1.61 | 14.6 | 1.62 |
| 1.60_17 | | 16.5 | 1.66 | 16.4 | 1.65 |
| 1.60_19 | | 18.6 | 1.62 | 13.2 | 1.70 |

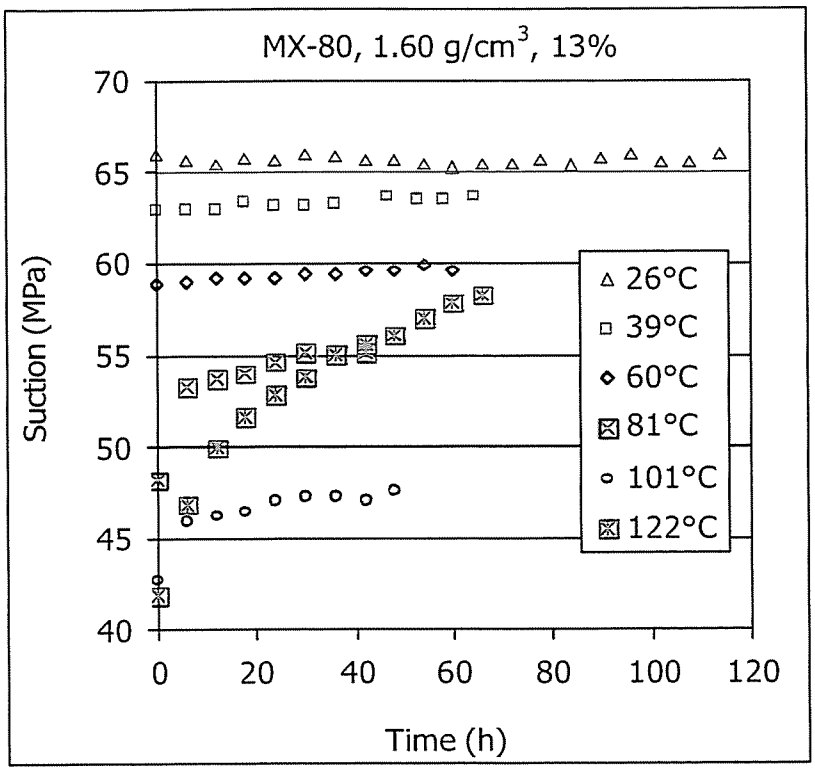


Figure 10: Evolution of suction measured on heating MX-80 bentonite compacted at 1.60 g/cm$^3$ with 13 percent water content (test 1.60_13)

Table IV: Equilibrium temperatures and suctions measured during heating/cooling of MX-80 bentonite compacted at nominal $\rho_d$ 1.60 g/cm$^3$ with different water contents (see Table III for actual values of $\rho_d$ and $w$)

| **160_11** | | **160_13** | | **160_15** | | **160_17*** | | **160_19** | |
|---|---|---|---|---|---|---|---|---|---|
| ***T*** **(°C)** | ***s*** **(MPa)** | ***T*** **(°C)** | ***s*** **(MPa)** | ***T*** **(°C)** | ***s*** **(MPa)** | ***T*** **(°C)** | ***s*** **(MPa)** | ***T*** **(°C)** | ***s*** **(MPa)** |
| 27 | 87 | 26 | 66 | 27 | 41 | 27 | 38 | 24 | 20 |
| 39 | 81 | 39 | 63 | 41 | 38 | 41 | 36 | 43 | 16 |
| 63 | 74 | 60 | 59 | 62 | 34 | 61 | 33 | 60 | 14 |
| 83 | 69 | 81 | 54 | 81 | 29 | 81 | 29 | 80 | 7 |
| 102 | 59 | 101 | 47 | 101 | 22 | 101 | 22 | 100 | 2 |
| 122 | 50 | | | 121 | 12 | 120 | 8 | | |
| 101 | 66 | | | 102 | 31 | 99 | 26 | | |
| 80 | 78 | | | 81 | 45 | 79 | 37 | | |
| 60 | 86 | | | 61 | 52 | 59 | 44 | | |
| 41 | 90 | | | 40 | 58 | 36 | 48 | | |
| 21 | 93 | | | 26 | 62 | 27 | 51 | | |

* $\rho_d$ of test 160_17 was 1.66 g/cm$^3$

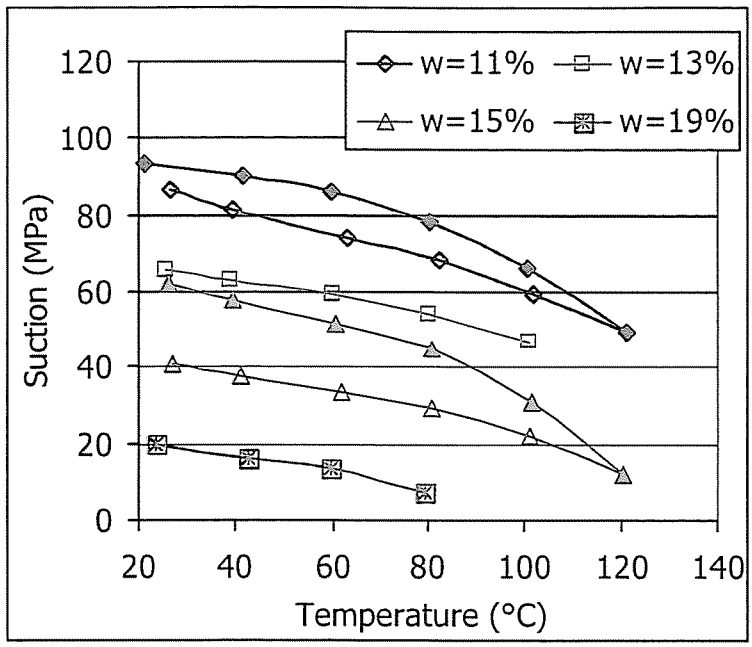


Figure 11: Equilibrium suction measured during heating/cooling in blocks of MX-80 bentonite compacted at 1.60 g/cm$^3$ with different water contents (bold symbols: cooling)

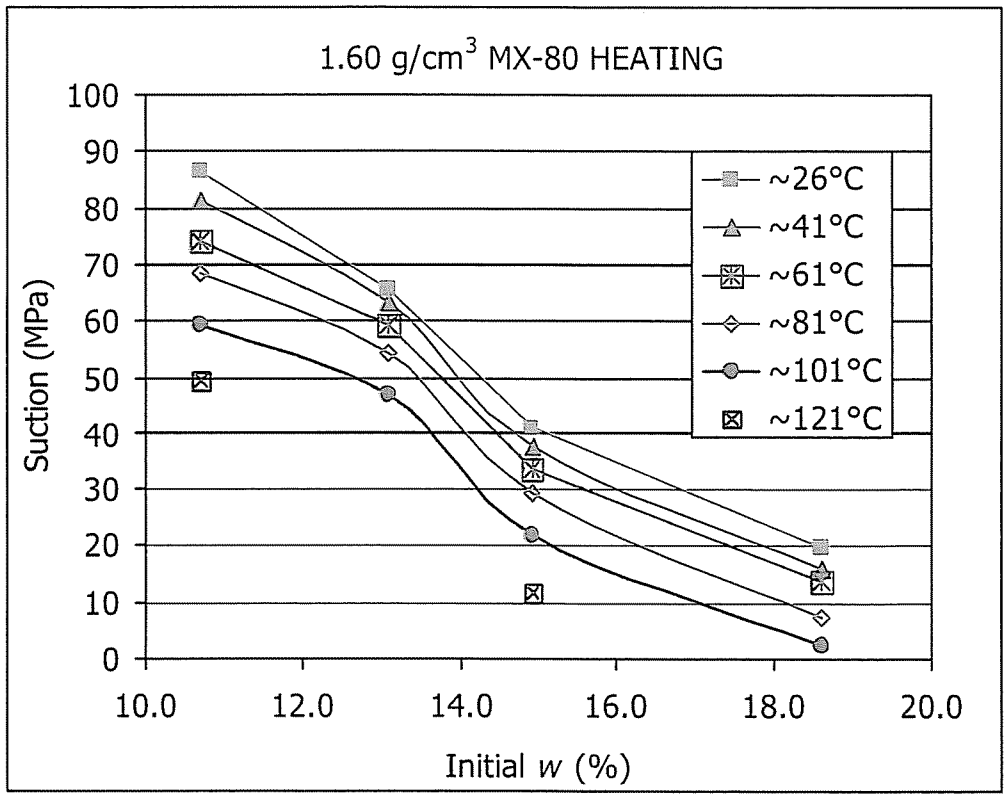


Figure 12: Retention curves obtained during heating with the sensor/cell method for the MX-80 bentonite compacted at 1.60 g/cm$^3$

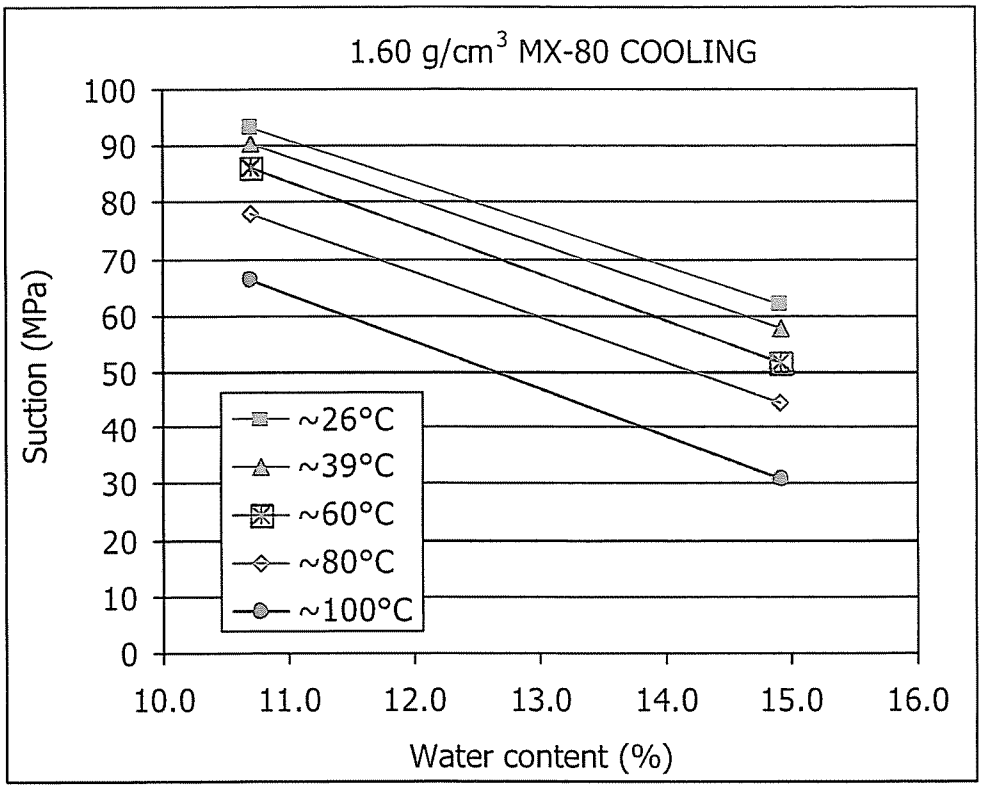


Figure 13: Retention curves obtained during cooling with the sensor/cell method for the MX-80 bentonite compacted at 1.60 g/cm$^3$

### 3.2.3 Discussion

The methodology designed to determine retention curves at high temperature has proven successful and easy to apply. The decrease of retention capacity with temperature has been checked for the two densities tested, both on heating and on cooling. As well, for a given temperature, the suction measured in a sample is higher when it is being cooled down than when it was being heated up, what is probably a consequence of microstructural changes taking place with temperature changes.

The effect of density on the retention capacity has also become clear. Figure 14 shows the results obtained during heating for blocks compacted to different dry densities with two water contents. For a given water content and temperature the suction measured in the high-density sample is higher. For suctions higher than 10 MPa, it has been observed for the FEBEX and the MX-80 bentonites that, for the same suction, the water content of samples compacted at higher density is slightly higher, whereas for suctions below this value, the trend reverses, *i.e.* samples compacted at higher density retain less water for a given suction.

Some of the results for the two densities are plotted together in Figure 15 in the form of retention curves. In terms of water content, the differences among densities become bigger towards the lower suctions, especially for the higher temperatures. At high suctions the water must be only in the microstructure, and since the density changes affect mainly the macrostructure, they are less reflected on the retention curve (Villar *et al.* 2005a).

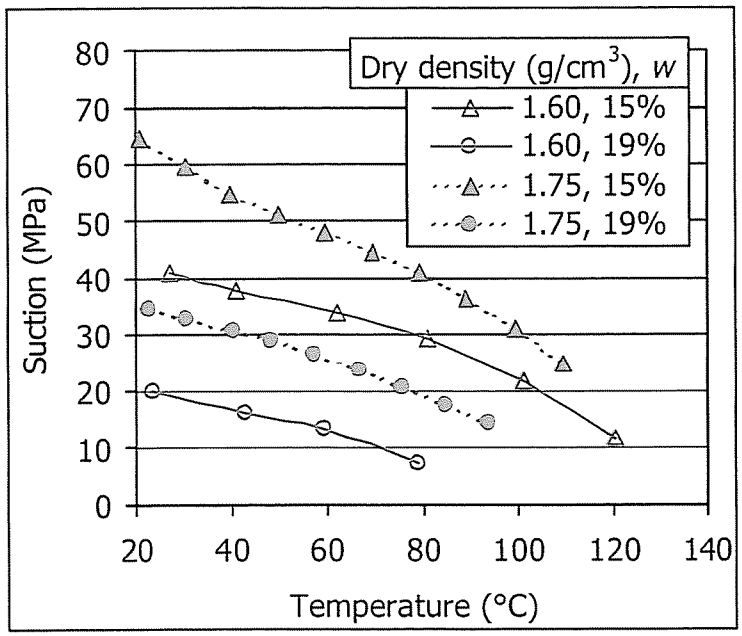


Figure 14: Suction measured during heating in blocks of MX-80 bentonite compacted at different dry densities with different water contents

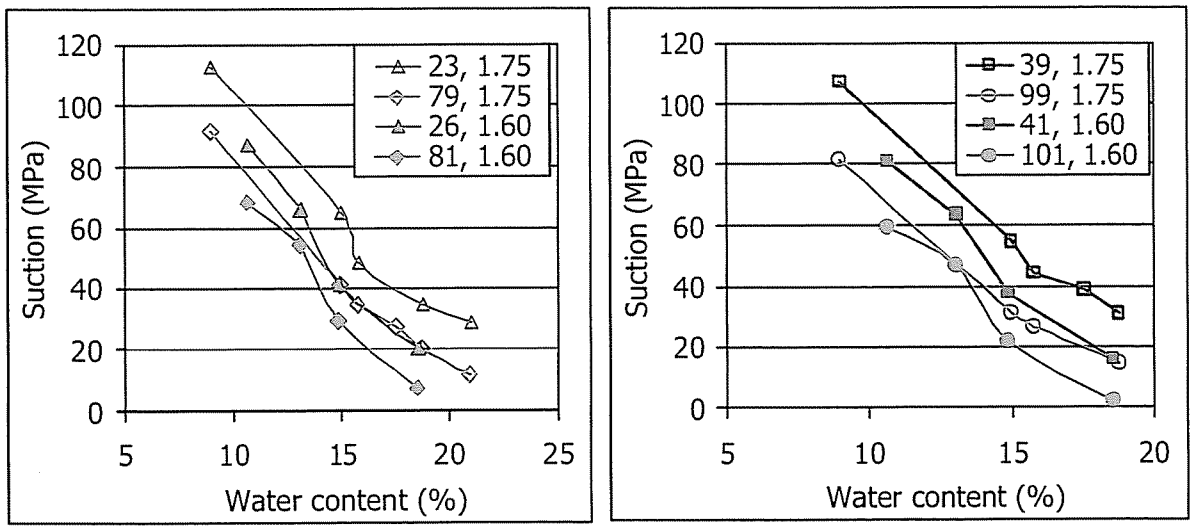


Figure 15: Retention curves at various temperatures (indicated in °C) for MX-80 bentonite compacted to different dry densities (indicated in g/cm$^3$)

The retention curves of MX-80 compacted at different densities were obtained in a previous investigation using perforated stainless steel cells placed in desiccators that keep constant relative humidities by means of sulphuric acid solutions (Villar 2005). The bentonite is compacted inside the cells, which remain in the desiccators until stabilisation of the water content of the bentonite, what is checked by weighing. If wetting paths are followed (by decreasing progressively the suction in the desiccators), the volume of the samples is kept constant during the determination because the cells cannot deform and swelling is avoided. This method is extremely time-consuming. In the curves obtained for MX-80 bentonite, the effect of wetting/drying hysteresis is not significant.

Figure 16 and Figure 17 show the results obtained with the cell method and with the sensor/cell method for the bentonite compacted at dry density 1.60 g/cm$^3$ at laboratory temperature and at 60°C, respectively. Figure 18 shows a comparison of the retention curves obtained with the cell method and with the sensor/cell method at a temperature of 60°C for the dry density of 1.75 g/cm$^3$. The agreement in all the cases is very good, with just a small deviation for the lower suctions. In the case of the higher densities (Figure 18) the deviation can be due to the fact that the densities are close but not the same: as expected, the sample with the lower density –the one tested with the sensor/cell method– tends to retain more water for the lower suctions (Villar 2002, Villar & Lloret 2004).

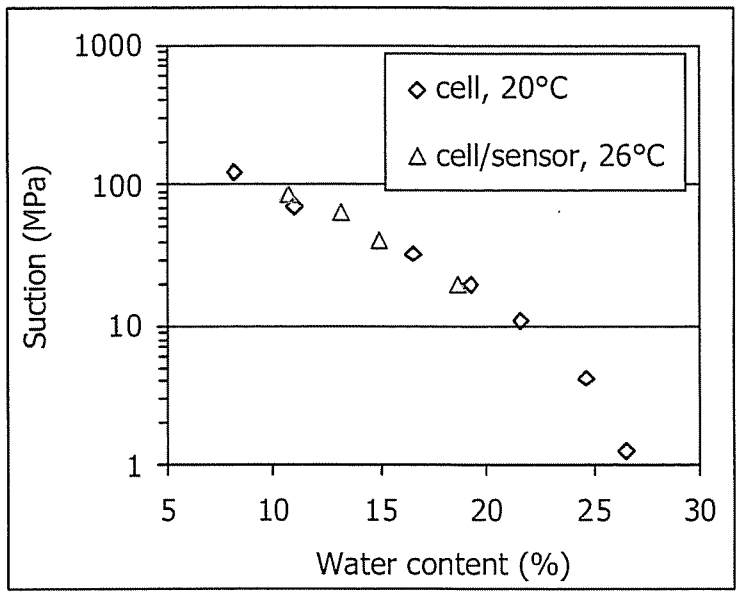


Figure 16: Retention curves obtained at laboratory temperature with two methods for the MX-80 bentonite compacted at 1.60 g/cm$^3$

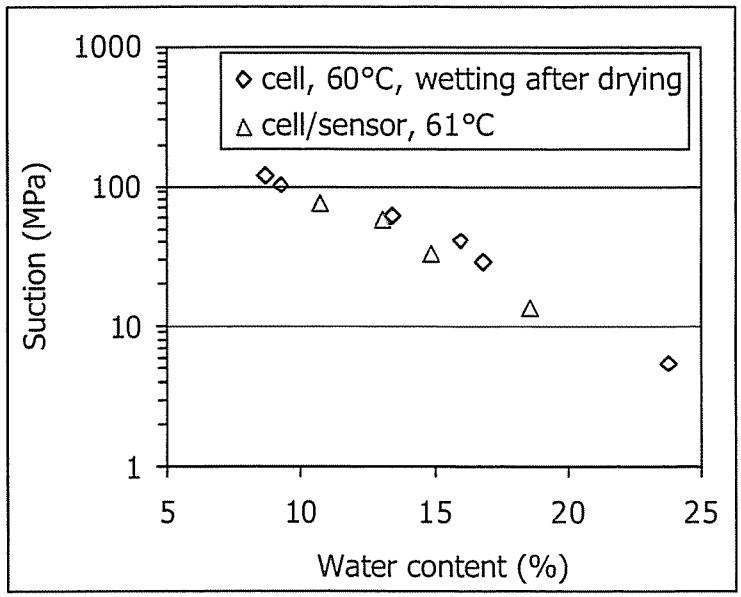


Figure 17: Retention curves obtained at 60°C with two methods for the MX-80 bentonite compacted at 1.60 g/cm$^3$

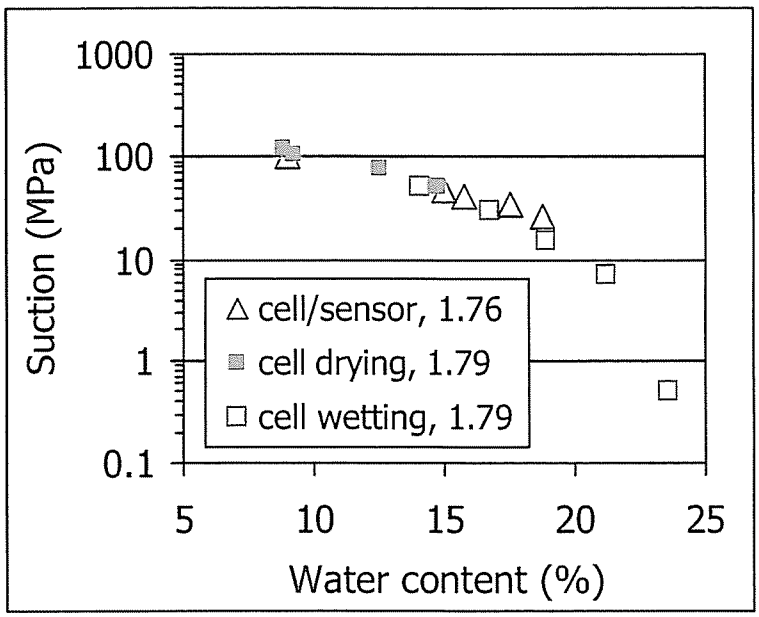


Figure 18: Retention curves obtained at 60°C with two methods for the MX-80 bentonite (dry density indicated in g/cm$^3$)

## 4. INFILTRATION TESTS

The infiltration tests submit the clay to conditions close to those at the barrier with respect to the thermal and hydraulic conditions and serve to analyse its behaviour. The bentonite is compacted to densities similar to those of the blocks of the large-scale TBT test and introduced in cylindrical cells. The bentonite is heated on the bottom while hydration with deionised water takes place by the upper part. Various cells have been used to perform these tests, since preliminary tests were conducted at the beginning. Also, two tests in which the bentonite was just hydrated have been carried out to check particular aspects of the model.

At the end of the tests, the water content and dry density of the bentonite at different levels along the block are determined. Water content is determined by oven drying at 110°C for 24 hours. To determine the dry density, the volume of the specimens is measured by immersing them in a recipient containing mercury and by weighing the mercury displaced.

A summary of the characteristics of the tests performed can be found in Table V, and a detailed description of each of them is given below.

Table V: Characteristics of the infiltration tests

| Test reference | TBT10_1* | TBT10_2 | TBT10_3 | TBT20_1 | TBT20_2 |
|---|---|---|---|---|---|
| **Nominal $\rho_d$ (g/cm$^3$)** | 1.75 | 1.60 | 1.60 | 1.70 | 1.70 |
| **Actual $\rho_d$ (g/cm$^3$)** | 1.74 | | | 1.67 | 1.70 |
| **Initial water content (%)** | 8.9 | 10.7 | 10.7 | 16.7 | 15.8 |
| **Height (cm)** | 10 | 10 | 10 | 20 | 20 |
| **Diameter (cm)** | 5 | 7 | 5 | 7 | 7 |
| **Injection pressure (MPa)** | 1.3 | 0.6 | 0.6 | 0.01 | 0.01 |
| **Lower temperature (°C)** | 100 | Room | Room | 140 | 140 |
| **Upper temperature (°C)** | Room | Room | Room | 30 | 30 |
| **Duration (h)** | 986 | 717 | 788 | 8087 | 11903 |

* bentonite from the first batch

### 4.1 Test TBT10_1

Test TBT10_1 was a heating/hydration preliminary test performed with bentonite from the first batch received at CIEMAT (hygroscopic water content 9 percent) compacted to nominal dry density 1.75 g/cm$^3$ (actual 1.74 g/cm$^3$).

It was performed in a cell made out of Teflon PTFE (Figure 19), whose thermal conductivity is 0.25 W/m·K. In order to reinforce mechanically the walls of the cell, that are to support the swelling pressure of the clay, the cell has an external steel casing. The internal diameter of the cell is 5 cm and the height 10 cm. The upper closing of the cell is made by means of a 316L stainless steel plug with lateral o-rings to close the cell. A central perforation allows the passage of the hydration water through it. The upper steel plug has concentric grooves machined on its bottom to help a better water distribution. A 5-cm diameter 316L stainless steel filter of 10-μm pore diameter and a filter paper are placed between the plug and the bentonite. The tightening of all the cell body and the upper closing is made by means of six external steel threaded bars and plates on top and bottom. The heating system, inserted at the Teflon bottom of the cell, consists of a stainless steel circular heater. It is sealed by an o-ring at the bottom and is pressed against the base of the cell by means of a piston rod, which is tightened by means of a knurled nut in the outside of the cell. The cables of the control K-type thermocouple and of the power supply pass through the piston rod. The temperature control is constituted by a PID temperature controller that regulates a solid state relay, enabling or disabling the power output towards the resistance, according to the temperature reached. The controller has a function of automatic PID regulation that remains activated. The resistance is fed by a 24 VAC transformer.

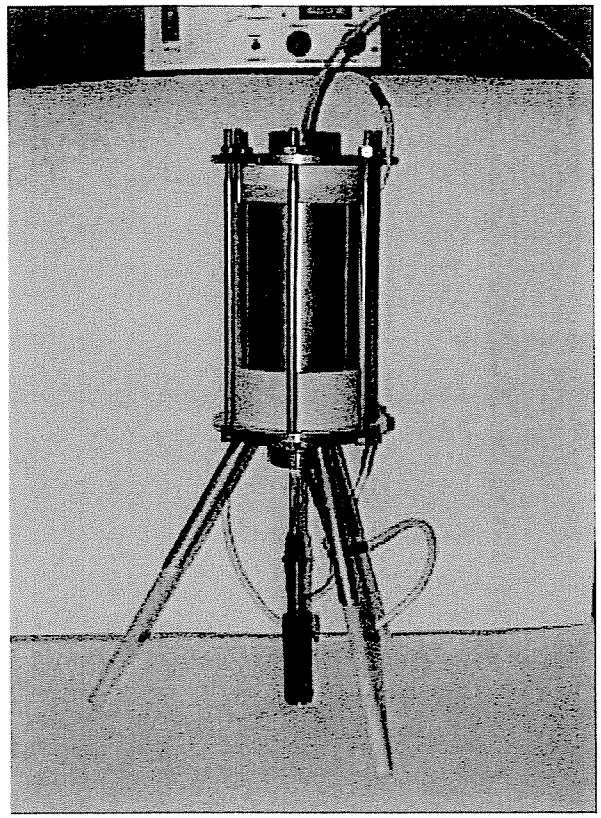

Figure 19: Teflon cell mounted to perform heating-hydration tests

Four 2.5-cm height bentonite blocks were uniaxially compacted at a nominal dry density of 1.75 g/cm$^3$ and piled into the cell. Once the cell mounted the heater temperature was set to 100°C and after 24 h the hydration system was connected. Deionised water was injected through a piston pump at a pressure of 1.3 MPa. The water intake was measured by means of an automatic volume change apparatus with an LVDT displacement transducer that allows measuring changes of volume with an accuracy of 0.001 cm$^3$. It is connected to a Data Acquisition System that records the water volume intake as a function of time.

The test run on for 40 days and the water intake measured is shown in Figure 20. According to this measurement, the total water intake at the end of the test was of 126 cm$^3$. However, upon dismantling it was checked by weight differences that the actual water intake of the bentonite block had been of just 61 cm$^3$, which corresponds to a final water content of 17.9 percent. This indicates either that the cell did not remain airtight and evaporation took place during hydration, or that the water intake measurement was faulty. The final distribution of water content and dry density are shown in Figure 21 and Table VI.

The decrease of water content with respect to the initial one in the zone closer to the heater is remarkable, as well as the increase of dry density in the same area. On the other hand, the water content increase near the hydration surface gave place to a noticeable decrease of dry density.

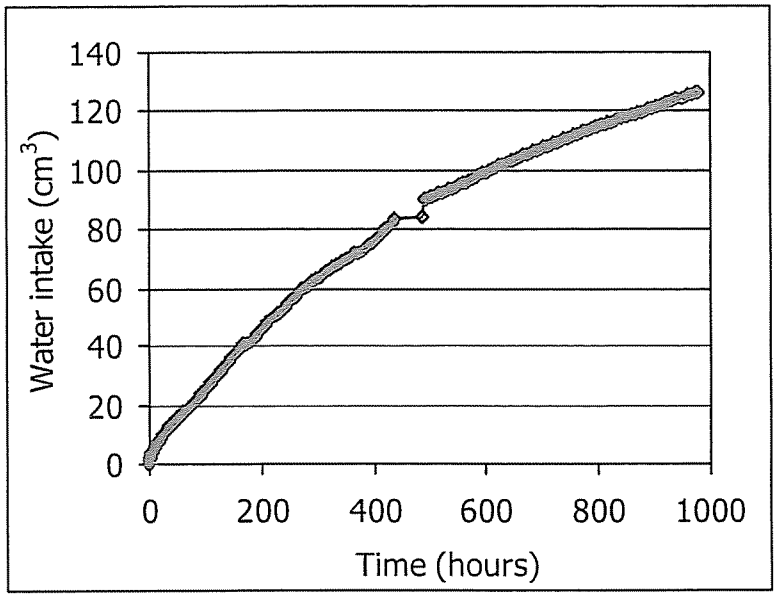


Figure 20: Water intake in test TBT10_1 (including evaporation)

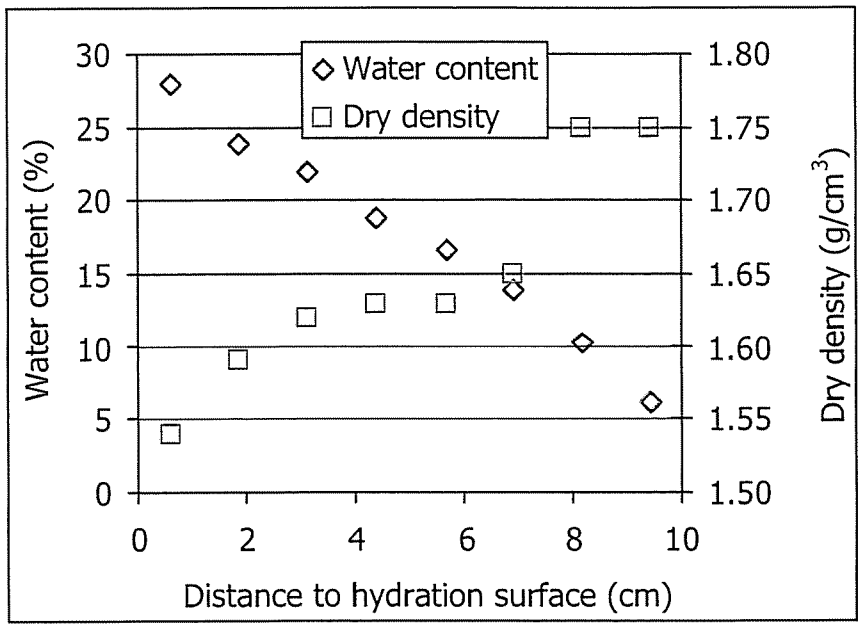


Figure 21: Final distribution of water content and dry density in test TBT10_1

Table VI: Final water content and dry density in test TBT10_1

| Position* (cm) | $w$ (%) | $\rho_d$ (g/cm$^3$) | $S_r$ (%) |
|---|---|---|---|
| 0.63 | 27.6 | 1.54 | 94 |
| 1.89 | 24.0 | 1.59 | 87 |
| 3.15 | 21.6 | 1.62 | 82 |
| 4.41 | 18.8 | 1.63 | 73 |
| 5.67 | 16.6 | 1.63 | 64 |
| 6.93 | 13.8 | 1.65 | 55 |
| 8.19 | 10.4 | 1.75 | 48 |
| 9.45 | 6.2 | 1.75 | 28 |
| Average | 17.2 | 1.65 | 68 |

*distance to hydration surface

## 4.2 Test TBT10_2

Test TBT10_2 is a hydration test performed at laboratory temperature in a stainless steel cell of internal diameter 7 cm and height 10 cm (Figure 2). The cell was modified to allow hydration through the upper cover. The bentonite with its hygroscopic water content (11 percent) was compacted in a single block of nominal dry density 1.60 g/cm$^3$ that was later placed in the cell. A uniaxial pressure of 29 MPa was applied to manufacture the block. Due to the friction of the piston with the mould walls during compaction a density gradient is generated, with higher densities on top.

Deionised water was injected on top of the bentonite by means of an oil/water pressure system at a pressure of 0.6 MPa during 30 days. Geotextile and filter paper discs were put between the cover of the cell and the bentonite. The measurement of water intake during the test was invalid. The final water content determined taking into account the difference between the final and initial weight of the bentonite was 18.0 percent. The final distribution of water content and dry density along the bentonite block is shown in Figure 22 and Table VII. The water content has increased all along the bentonite down to the bottom of the cell. However, the dry density distribution seems to reflect the gradient generated during compaction, that has not been obliterated during hydration, except in the upper part of the bentonite, where the significant water content increase has induced intense swelling and density diminution. Figure 23 shows the final appearance of the bentonite, the darker colour of the highly-saturated upper part being remarkable.

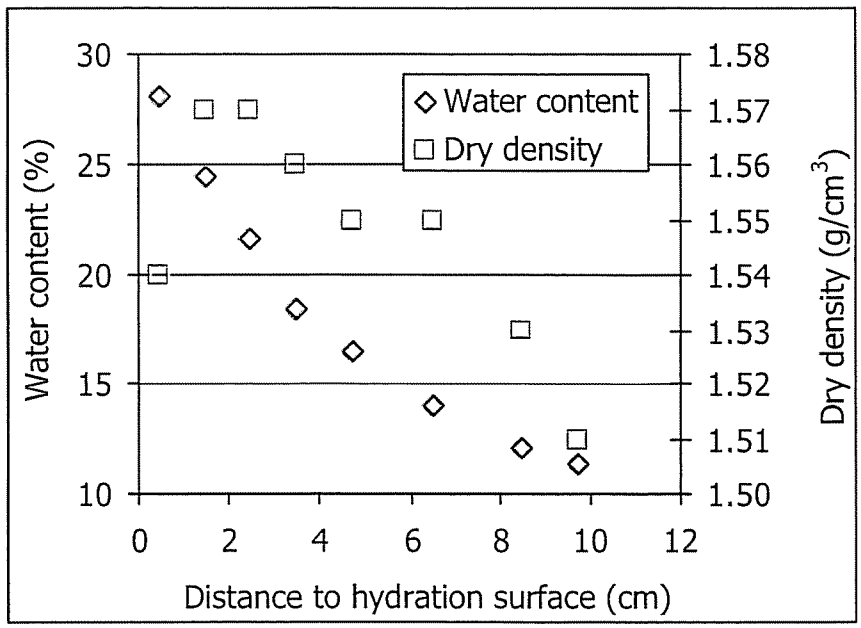


Figure 22: Final distribution of water content and dry density in test TBT10_2

Table VII: Final water content and dry density in test TBT10_2

| **Position* (cm)** | $w$ (%) | $\rho_d$ (g/cm$^3$) | $S_r$ (%) |
|---|---|---|---|
| 0.50 | 28.1 | 1.54 | 95 |
| 1.50 | 24.5 | 1.57 | 87 |
| 2.50 | 21.6 | 1.57 | 77 |
| 3.50 | 18.5 | 1.56 | 65 |
| 4.75 | 16.5 | 1.55 | 57 |
| 6.50 | 14.0 | 1.55 | 48 |
| 8.50 | 12.1 | 1.53 | 40 |
| 9.75 | 11.4 | 1.51 | 37 |
| Average | 18.3 | 1.55 | 63 |

*distance to hydration surface

Figure 23: Final appearance of the bentonite block of test TBT10_2

### 4.3 Test TBT10_3

Test TBT10_3 is a hydration test performed at laboratory temperature in the Teflon cell described in section 4.1 (Figure 19). The heater was not switched on and the cell was placed on a balance in order to have a cross-checking of the water intake measurement performed by the automatic volume change apparatus.

Four blocks 2.5-cm diameter and 5.0-cm height were obtained by uniaxial compaction of the clay with its hygroscopic water content (11 percent) to dry density 1.60 g/cm$^3$. The pressure applied to manufacture each block was 21 MPa.

Deionised water was injected on top of the bentonite by means of an oil/water pressure system at a pressure of 0.6 MPa during 33 days. The measurements of water intake done by the volume change apparatus and by the balance were coherent during the test. There were some problems in the automatic volume recordings at the beginning of the test, as shown in Figure 24. The total water intake according to this measurement was 21 cm$^3$, whereas the difference between the final and initial weight of the bentonite was 20 g, what allows considering the water intake evolution shown in Figure 24 as correct.

The appearance of the bentonite after dismantling is shown in Figure 25, where it can be appreciated that the two upper blocks became sealed during hydration. Figure 26 and Table VIII show the distribution of water content and dry density of the bentonite at the end of the test. There is a gradual increase of water along the bentonite, more pronounced in the upper part but also reaching the bottom of the sample. The water content change in the upper block is remarkable (Figure 27), with the first 0.5 cm reaching a water content of 30 percent, what gives place to important swelling and diminution of dry density to 1.46 g/cm$^3$.

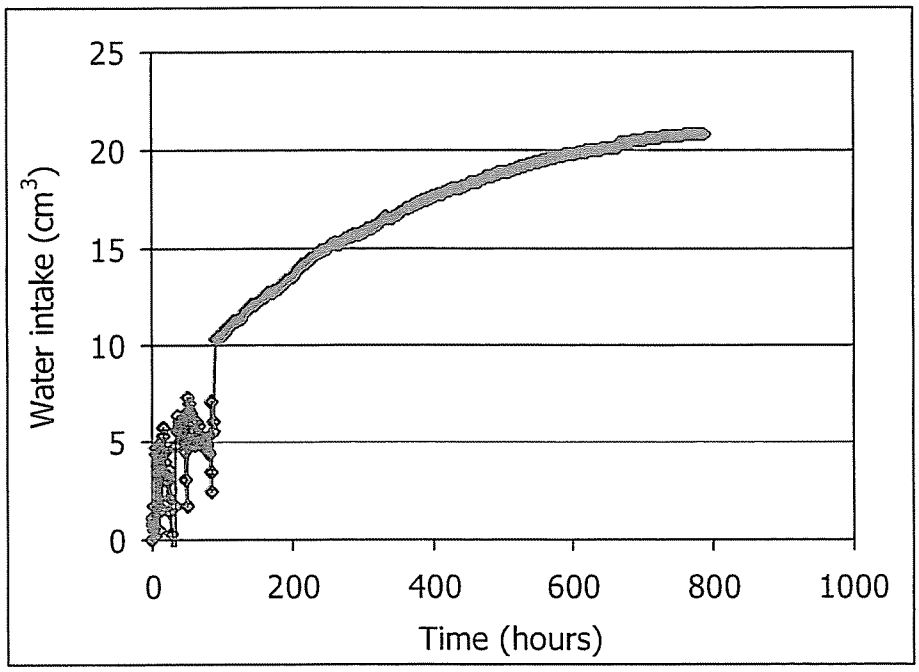


Figure 24: Water intake in test TBT10_3

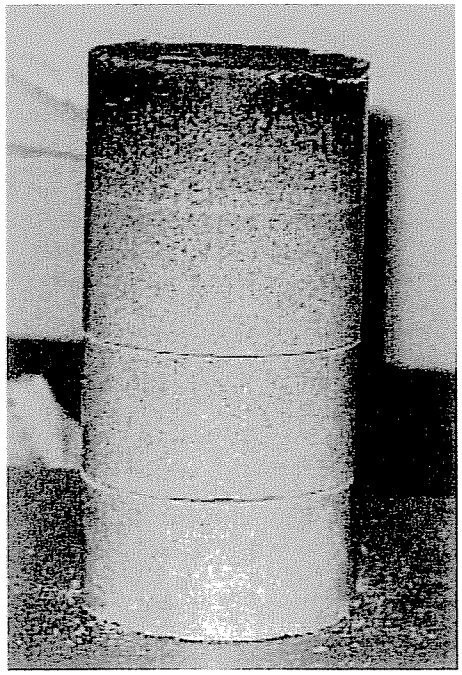

Figure 25: Final appearance of the bentonite blocks of test TBT10_3

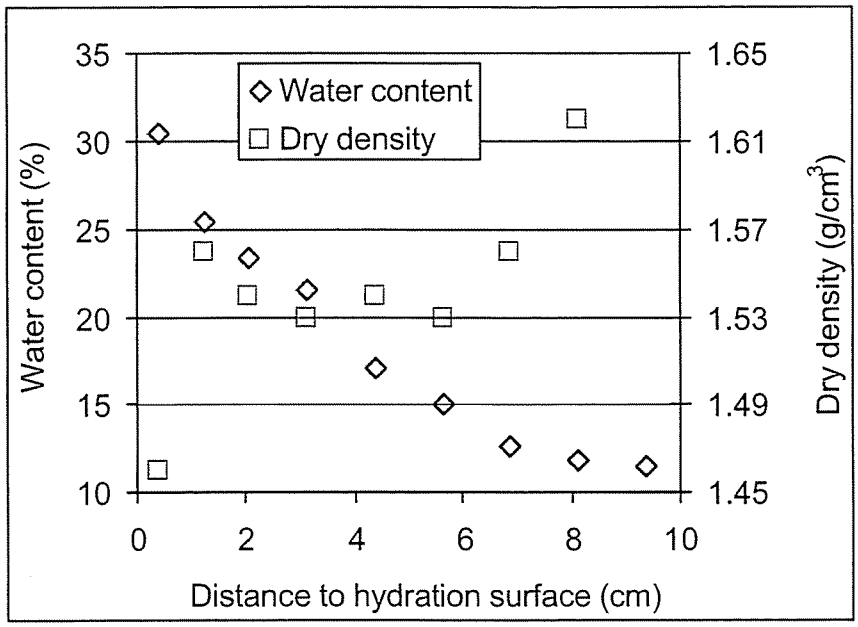


Figure 26: Final distribution of water content and dry density in test TBT10_3

Table VIII: Final water content and dry density in test TBT10_3

| **Position* (cm)** | $w$ (%) | $\rho_d$ (g/cm$^3$) | $S_r$ (%) |
|---|---|---|---|
| 0.40 | 30.4 | 1.46 | 92 |
| 1.25 | 25.4 | 1.56 | 89 |
| 2.05 | 23.4 | 1.54 | 79 |
| 3.13 | 21.6 | 1.53 | 72 |
| 4.38 | 17.0 | 1.54 | 58 |
| 5.63 | 15.0 | 1.53 | 50 |
| 6.88 | 12.6 | 1.56 | 44 |
| 8.13 | 11.8 | 1.62 | 45 |
| 9.38 | 11.5 | 1.62 | 44 |
| Average | 18.7 | 1.56 | 60 |

*distance to hydration surface

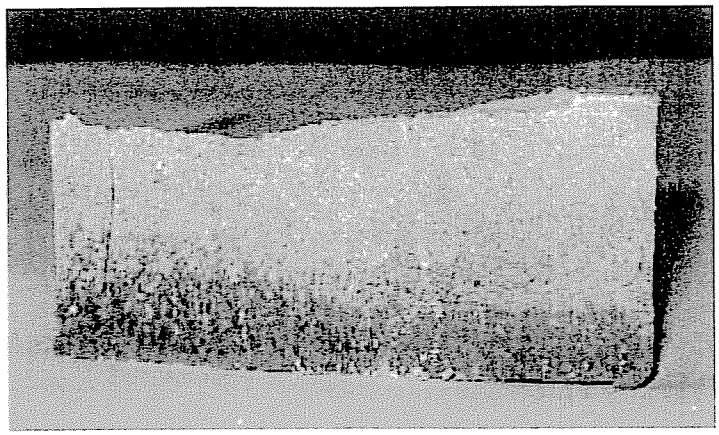

Figure 27: Final appearance of the upper bentonite block of test TBT10_3 (the block is upside down, *i.e.* the part in contact with the hydration surface is at the bottom of the picture)

### 4.4 Test TBT20_1

Test TBT20_1 was performed in a cylindrical cell, modified from cells already used during FEBEX I (Villar *et al.* 2005b), whose internal diameter is 7 cm and inner length 20 cm. It is made out of Teflon to prevent as much as possible lateral heat conduction, and externally covered with steel semi-cylindrical pieces to avoid the deformation of the cell by bentonite swelling.

Two 10-cm long blocks of MX-80 bentonite compacted with a water content of 17 percent at a nominal dry density of 1.70 g/cm$^3$ (actual 1.67 g/cm$^3$) were piled up inside the cell. Deionised water was injected through the upper lid of the cell at a pressure of 0.01 MPa (a 1-m water column). The bottom part of the cell is a plane stainless steel heater set at a temperature of 140°C, which is the temperature on the surface of the heater of the large-scale TBT test. Inside the upper steel plug of the cell there is a deposit in which water circulates at constant temperature (30°C). In this way, a constant gradient of 5.5 °C/cm between top and bottom of the sample is imposed. A schematic diagram of the setup is shown in Figure 28.

The body of the cell is constituted by a 200-mm length cylindrical piece (Figure 29, item 4) and a base (Figure 29, item 1). In order to avoid the heat dissipation as far as possible, all of them are made out of Teflon PTFE, whose thermal conductivity is 0.25 W/m·K. The thickness of the cell wall is 15 mm, and the pieces are assembled into each other. The watertightness of the contacts between different pieces is guaranteed by means of Viton® o-rings capable of withstanding temperatures of up to 180°C. In order to reinforce mechanically the walls of the cell, that are to support the swelling pressure of the clay, they have been externally surrounded by two pairs of 4-mm thickness 316L stainless steel shells (Figure 29, item 5), joint by steel braces (Figure 29, item 16). The vertical separation between pairs of shells is made by means of a Teflon PTFE ring, to break the heat transmission in longitudinal sense (Figure 29, item 6). The walls of the cells are provided with drillings for the installation of instrumentation.

The upper closing of the cell is made by means of a set made out of 316L stainless steel (Figure 29, item 7), consisting of a plug with lateral o-rings (Figure 29, item 8) to close the cell that includes a chamber for the cooling system. A central perforation allows the passage

of the hydration water through the chamber screwed cap (Figure 29, item 14) and through the plug (Figure 29, item 13). The upper steel plug has concentric grooves machined on its bottom.

The tightening of all the pieces is made by means of six external steel threaded bars and plates on top and bottom (Figure 29, items 11, 9 and 10). These bars serve as well as support of the cell (Figure 29, items 11 and 17).

The cell was instrumented with capacitive-type sensors placed inside the clay at three different levels, at 4, 9 and 14 cm from the hydration surface. The transmitters used are VAISALA HMP237 (Figure 31), which include a humidity sensor (HUMICAP®) that changes its dielectrical characteristics with extremely small variations in humidity (capacitive-type relative humidity (*RH*) sensor). They include also a temperature sensing element (Pt 100). The accuracy of the humidity sensor is ±1 percent over the range 0-90 percent *RH* and ±2 percent over the range 90-100 percent *RH*. The *RH* values are converted to suction values through Equation 1. The transmitters are protected by cylindrical stainless steel filters.

The final appearance of the mounted cell is shown in Figure 30. The cell is laterally surrounded with a 15-mm thick dense foam material whose thermal conductivity is 0.04 W/m·K.

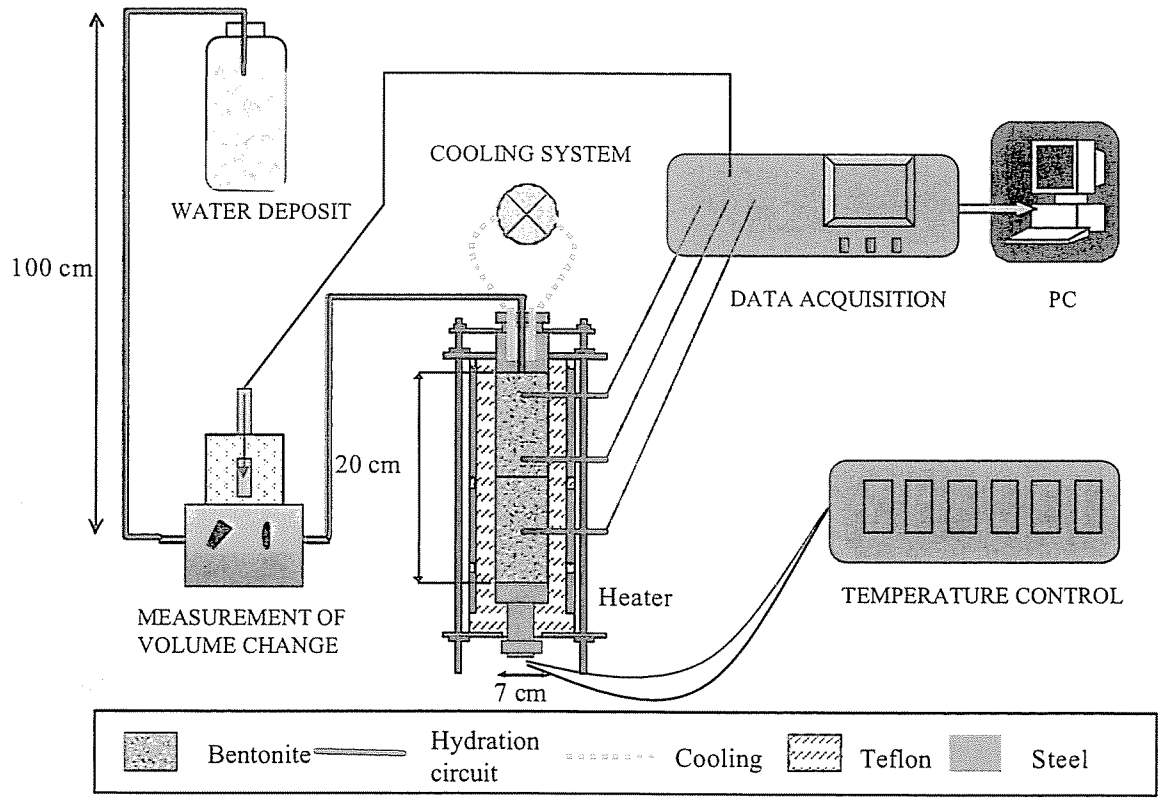


Figure 28: Experimental setup for the infiltration tests

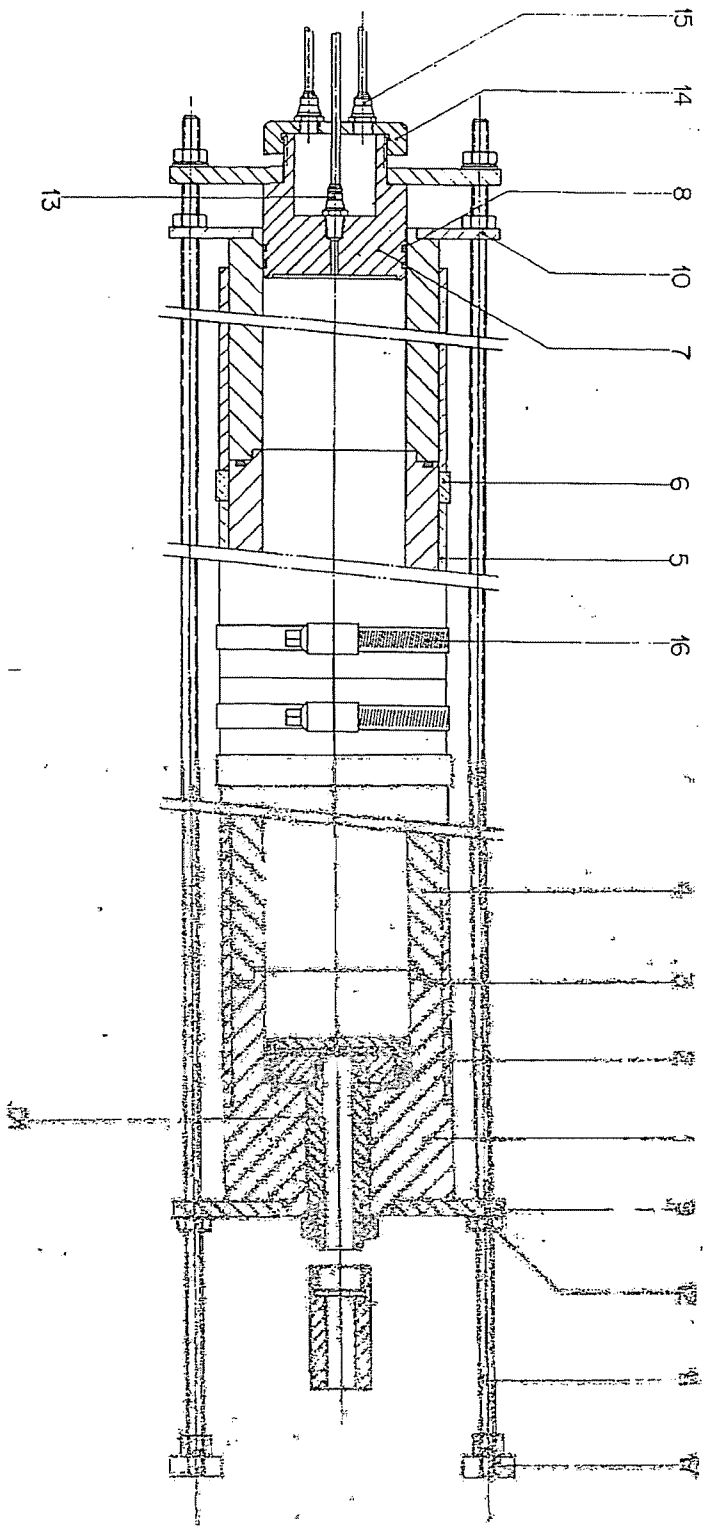


Figure 29: Cross section of the cell with its different components

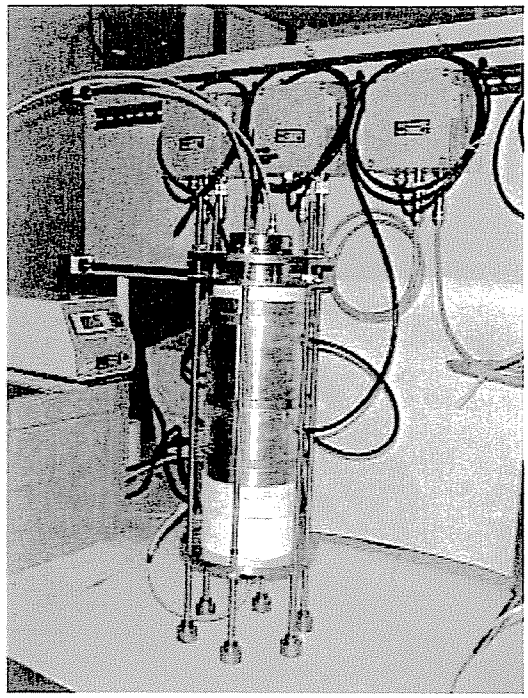

Figure 30: Appearance of the cell mounted for test TBT20_1

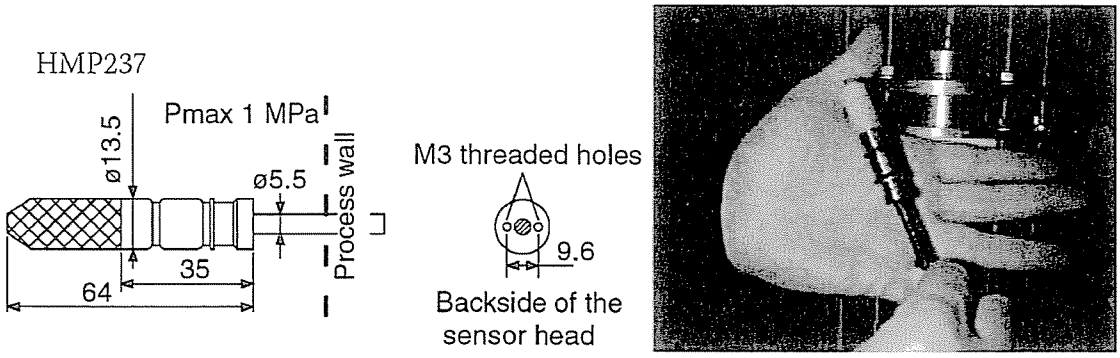


Figure 31: Vaisala HMP237 relative humidity sensors

The hydration was made with deionised water taken from a deposit placed 1 m above the upper part of the cell. A stainless steel porous sinter and a filter paper are placed in contact with the bentonite to help a better water distribution. An dectronic equipment for the measurement of water intake volume is placed at the entrance of the cell. It has an LVDT displacement transducer that allows measuring changes of volume with an accuracy of 0.001 $cm^3$.

A uniaxial pressure of 42 MPa was applied to manufacture the blocks. The thermal and hydraulic gradients were applied almost simultaneously: first the hydration system was connected, five minutes afterwards the cooling system was set, and after 10 more minutes the bottom heater was switched on. Figure 32 shows the evolution of relative humidity and temperature inside the clay in the first hours. The heater temperature is also shown in the figure, it can be seen that it took about 5 h to reach the target temperature of 140°C at the heater surface. After 10 h the temperatures inside the clay had almost reached steady values.

Since the initial water content of the clay was high (17 percent) the initial relative humidity inside the clay is also high (72 percent, corresponding to a suction of 44 MPa). Upon heating, the relative humidity at 6 cm from the heater (sensor 3) increases sharply after 0.5 h, up to more than 93 percent. This increase is probably due to the migration of water in the vapour phase coming from the bentonite closer to the heater. After 2.5 h this sensor seems to be flooded and the readings given are weird. Six hours after the beginning, the relative humidity remains constant and close to 90 percent. The sensor placed at 11 cm from the heater (sensor 2) did not record any relative humidity change for about 1 h. Afterwards it reflected a steady relative humidity increase that stabilises after 8 h around 90 percent. This increase is probably caused by the arrival of the water vapour front generated near the heater. The relative humidity at 16 cm from the heater (sensor 1) increases during the first half hour to 75 percent, probably by the effect of hydration. Then it stabilises for almost 2 h, and increases softly again. After 9 h stabilises in values close to 85 percent. The second increase could have been caused by the arrival of the water vapour front.

Assuming that a water vapour front is generated near the heater and migrates towards cooler zones, the moment in which the sensors start to record a relative humidity increase can be considered as the arrival of this front (for sensor 1, the second increase has been considered). This has been reflected in Figure 33.

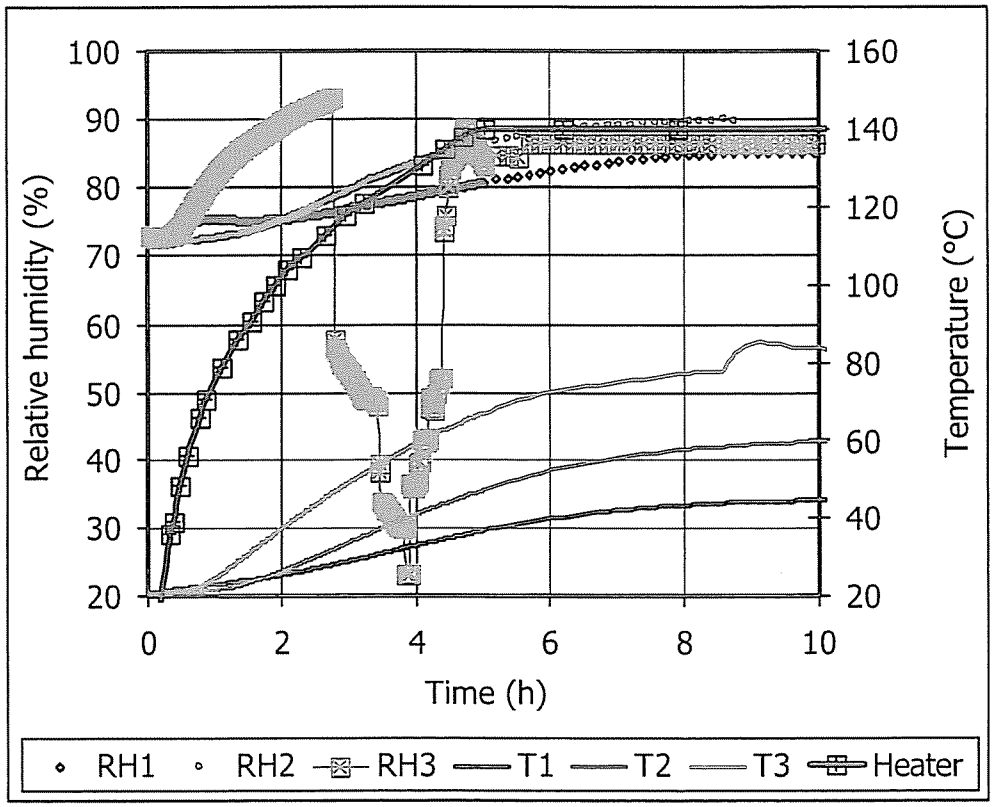


Figure 32: Evolution of temperature of the heater and of relative humidity and temperature of the bentonite at the beginning of test TBT20_1 (sensor 1 placed at 4 cm from the hydration surface, sensor 2 at 9 cm and sensor 3 at 14 cm)

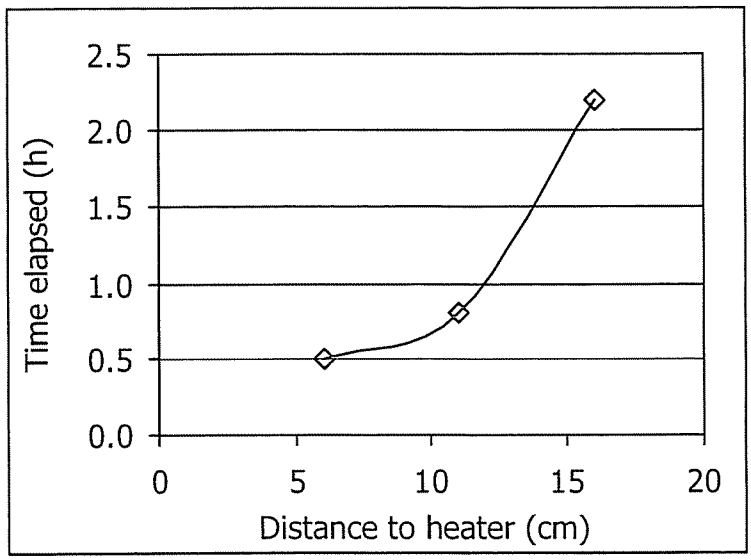


Figure 33: Time taken by the water vapour front to reach different zones of the bentonite

Figure 34 shows the evolution of temperature in three positions inside the bentonite during the test. After the first sharp increase, the temperature recorded by the lower sensor (sensor 3) decreased to values around 77°C. For the other sensors, the values reached at the beginning of the test remained quite constant over time, just reflecting the seasonal temperature variations of the laboratory. Sensor 1 failed after 5000 h.

Figure 35 shows the evolution of relative humidity recorded by the sensors during the test. Few hours after the starting of the test, the three sensors recorded erratic values, and finally seem to have been flooded.

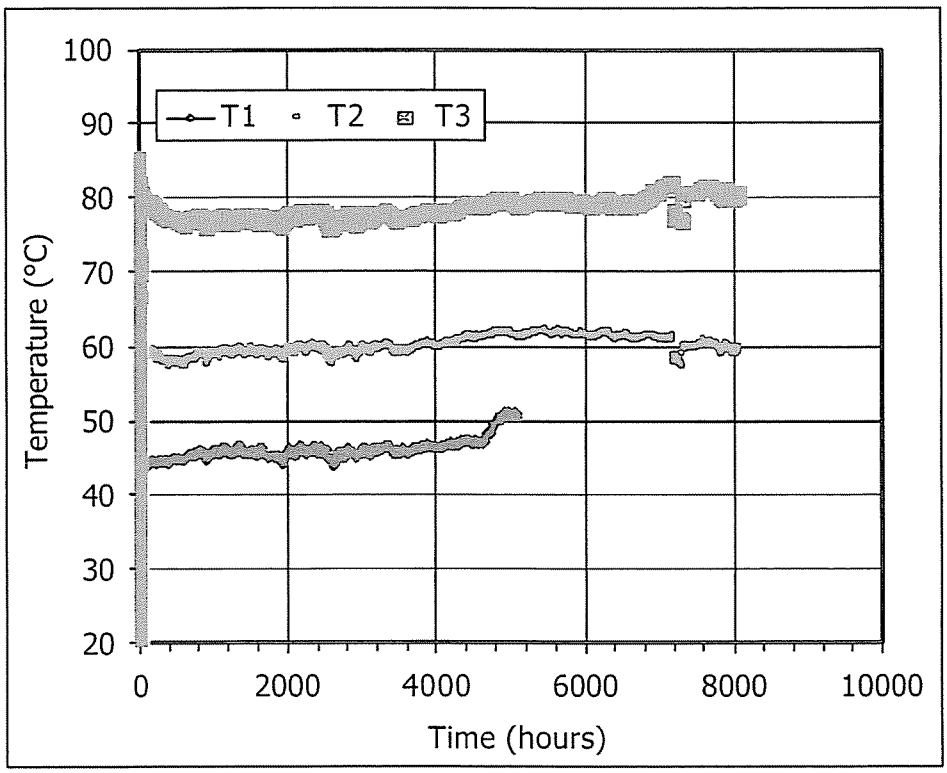


Figure 34: Evolution of temperature in test TBT20_1 (sensor 1 placed at 4 cm from the hydration surface, sensor 2 at 9 cm and sensor 3 at 14 cm)

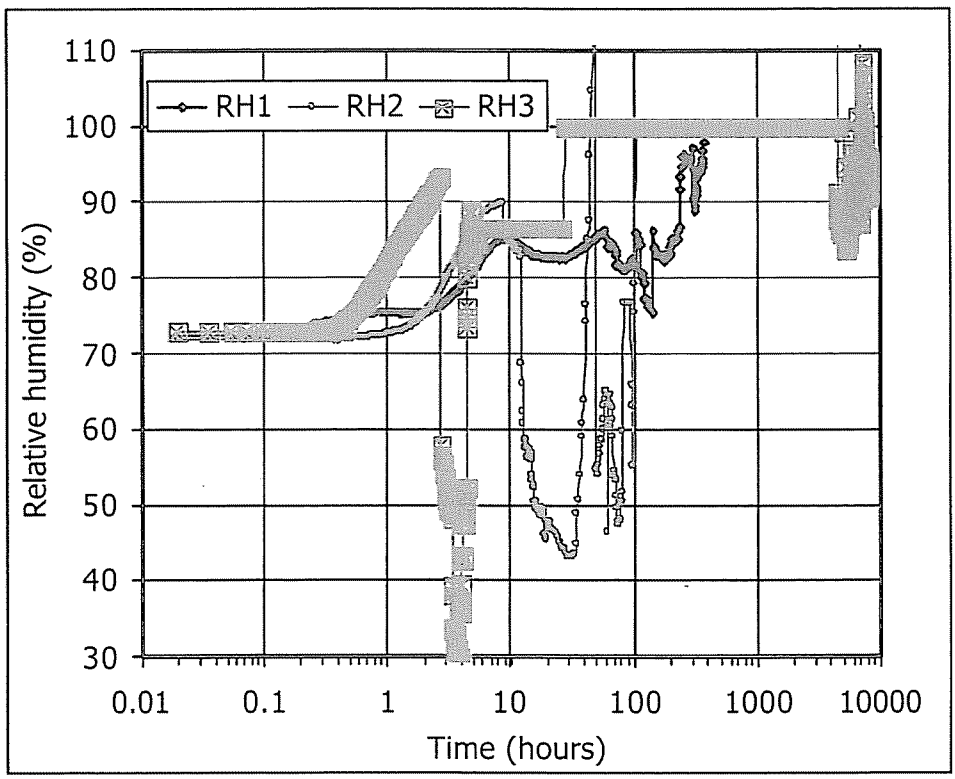


Figure 35: Evolution of relative humidity in test TBT20_1 (sensor 1 placed at 4 cm from the hydration surface, sensor 2 at 9 cm and sensor 3 at 14 cm)

The test went on for 337 days. Figure 36 shows the water intake measured by the volume change apparatus during the test. According to this measurement, the final water intake was of 142 $cm^3$. Upon dismantling, it was checked by weight differences that the actual water intake had been of just 28 g. Besides, the determination of water content along the bentonite reflected an intense drying, as can be seen in Figure 37 and Table IX. In fact, the final water content distribution was linear, from 34 percent near the hydration surface, to 1 percent near the heater, with an average value of 19 percent. The final appearance of the bentonite blocks reveals this drastic change in water content along the block (Figure 38). Cracks appeared in the drier bentonite on decompressing (Figure 39). Corrosion was noticeable in the upper surface of the lower bentonite block (Figure 40) and in the lower sensor (Figure 41). The dry density along the bentonite changed accordingly, decreasing in the hydrated areas and increasing near the heater. Thus, either the water intake measured was faulty, or evaporation outside the cell was taking place.

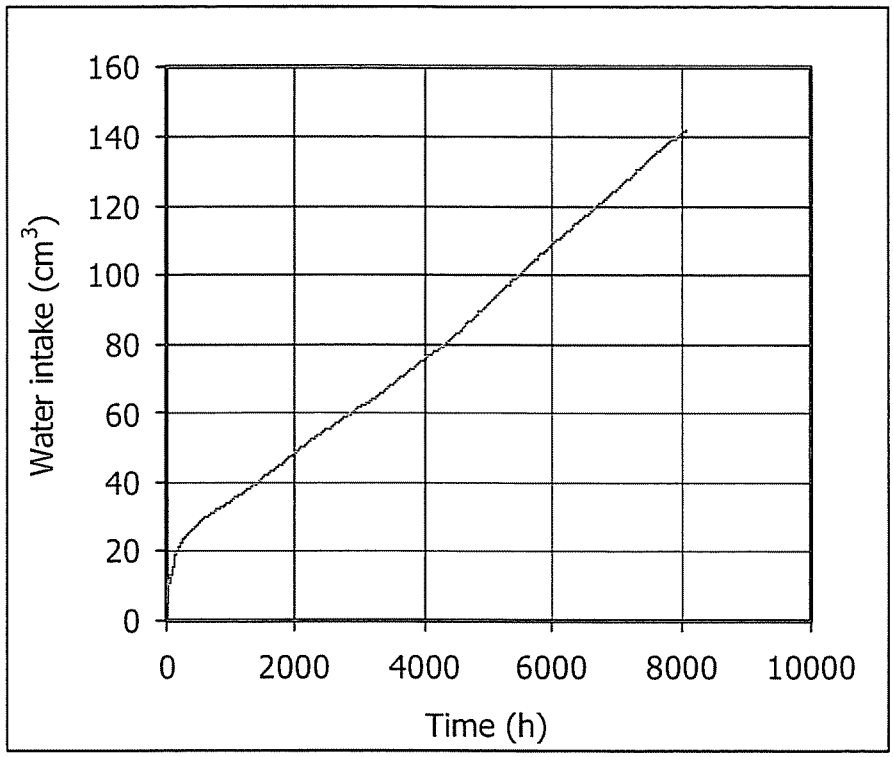


Figure 36: Water intake measured during test TBT20_1 (including evaporation?)

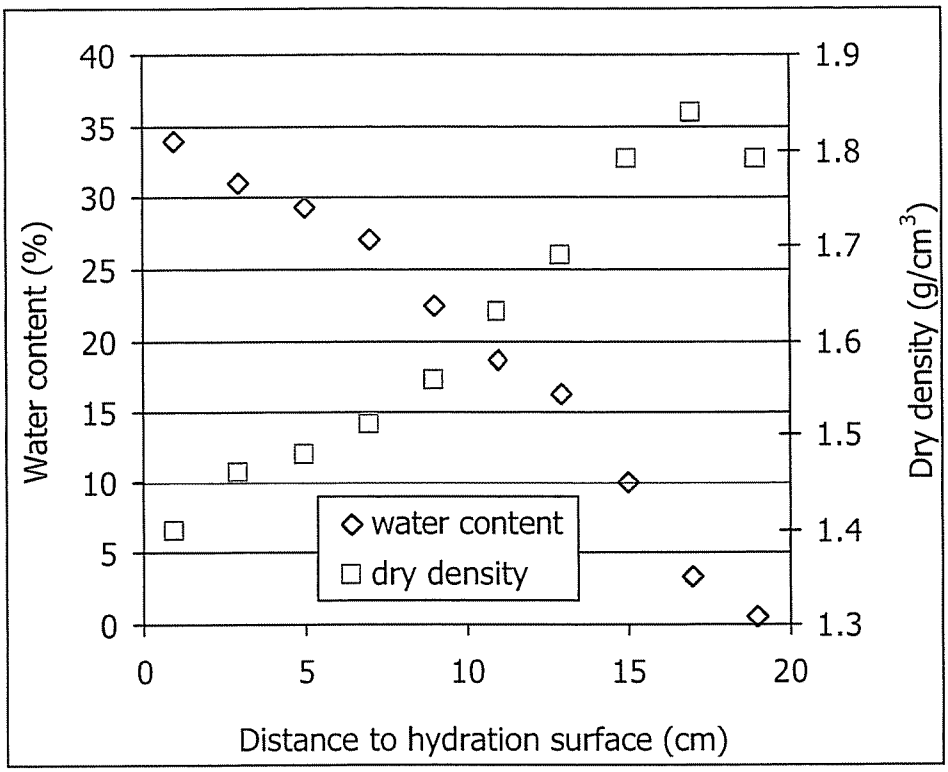


Figure 37: Final distribution of water content and dry density in test TBT20_1

Table IX: Final water content and dry density in test TBT20_1

| **Position* (cm)** | ***w* (%)** | **$\rho_d$ (g/cm$^3$)** | **$S_r$ (%)** |
|---|---|---|---|
| 1 | 33.9 | 1.40 | 94 |
| 3 | 31.0 | 1.46 | 94 |
| 5 | 29.3 | 1.48 | 91 |
| 7 | 27.1 | 1.51 | 88 |
| 9 | 22.5 | 1.56 | 79 |
| 11 | 18.7 | 1.63 | 72 |
| 13 | 16.3 | 1.69 | 69 |
| 15 | 9.9 | 1.79 | 49 |
| 17 | 3.4 | 1.84 | 18 |
| 19 | 0.6 | 1.79 | 3 |
| Average | 19.3 | 1.62 | 73 |

*distance to hydration surface

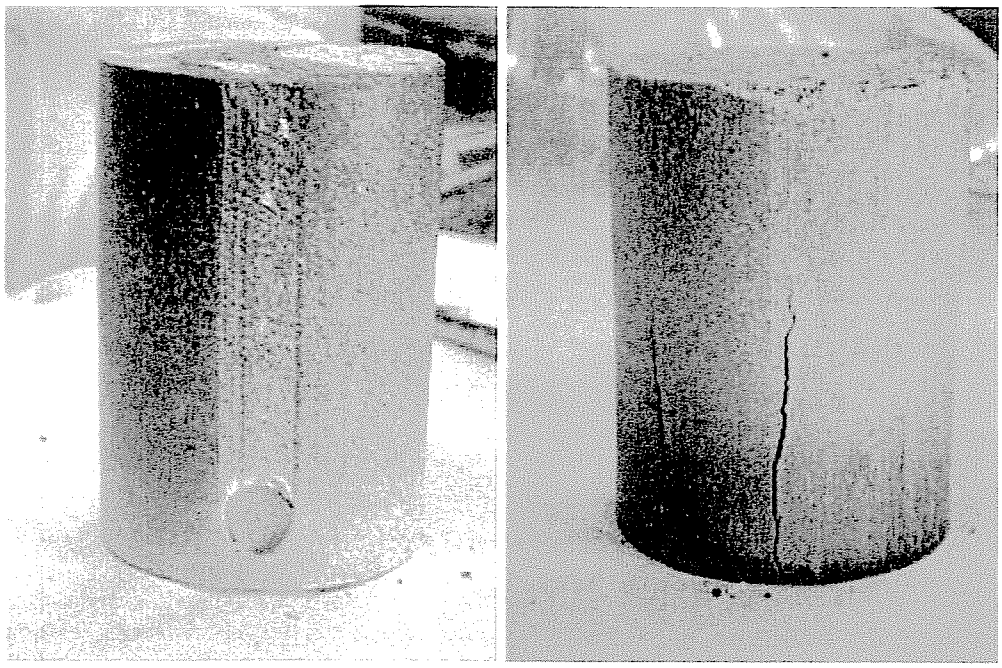

Figure 38: Final appearance of the upper (left) and lower (right) blocks of test TBT20_1

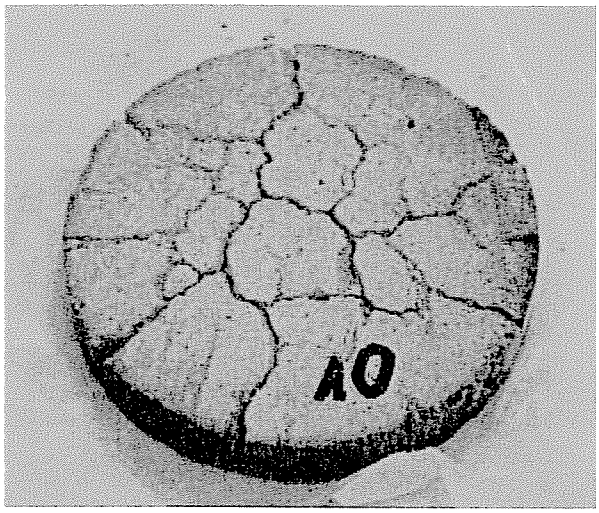


Figure 39: Appearance of the bentonite in contact with the heater at the end of test TBT20_1

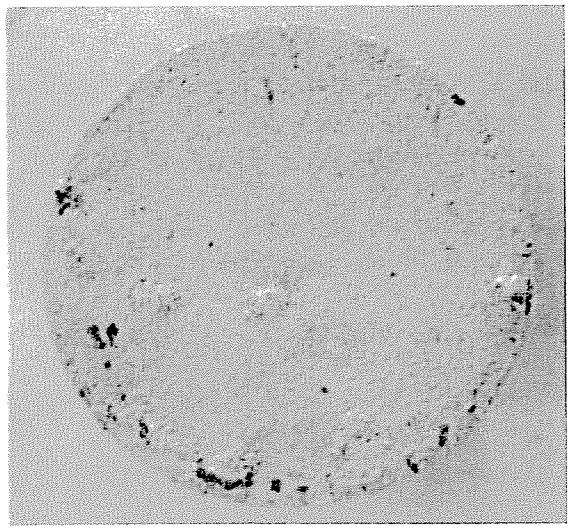

Figure 40: Appearance of the upper surface of the lower bentonite block at the end of test TBT20_1

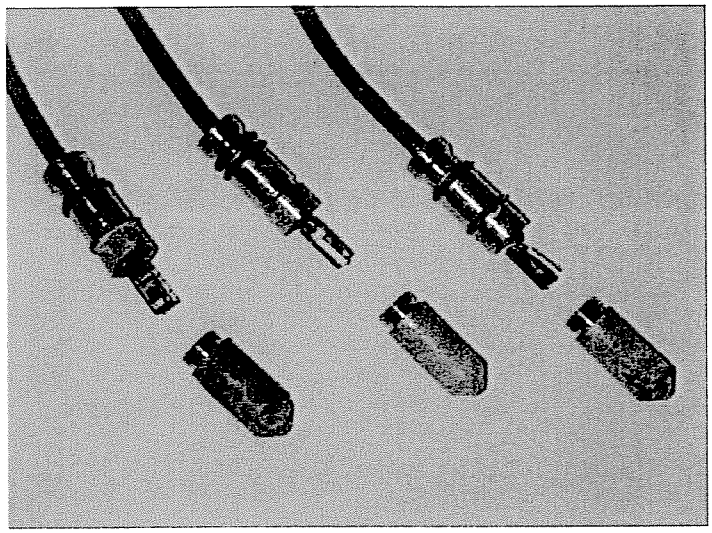

Figure 41: Final appearance of the sensors inserted in the bentonite in test TBT20_1 (left: upper sensor, right: lower sensor with corrosion evidences)

## 4.5 Test TBT20_2

Test TBT20_2 was mounted in the cell described in the previous section. Special care was taken to seal any pathway for possible leak, in particular the sensor connections in the cell wall. The procedures followed and the equipment used were the same than for test TBT20_1, except in the following:

- The dry density of the bentonite inside the cell was 1.70 g/cm$^3$, and the initial water content 16 percent ($S_r$ = 67%). A uniaxial pressure of 43 MPa was applied to manufacture the blocks.

- A filter paper was placed by mistake between the two blocks.

- The stainless steel shells (Figure 29, item 5) were not placed over the Teflon to avoid as much as possible heat conduction. Instead several steel braces (Figure 29, item 16) were used to withstand the swelling pressure of the bentonite.

- The mounted cell was placed over a balance to check the water intake by a means other than the volume change measurement apparatus (Figure 42).

- The starting off sequence was as follows:

    1. Once the cell mounted, the temperature of the heater was set to 100°C.

    2. After 190 h the temperature of the heater was increased to the final target value of 140°C.

    3. The upper cooling at 30°C was launched after 647 h.

    4. Hydration with a 1-m deionised water column started after 667 h.

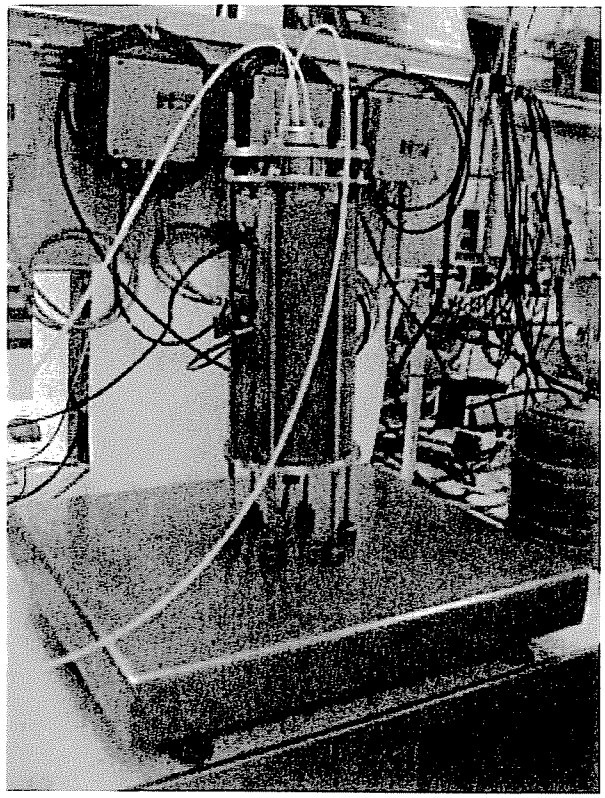

Figure 42: Experimental setup for test TBT20_2 (the cell is placed on a balance)

According to this procedure, the bentonite was initially heated during 28 days. The weight of the assemblage was checked daily so that to assure that no changes –and consequently leaks– took place. Figure 43 shows the recordings of the sensors during this initial heating phase. In less than 6 h after switching on the heater the temperatures inside the bentonite were

stabilised. The initial relative humidity recorded by the sensors was 67-68 percent, and upon heating it steadily increased in the areas in which sensors 1 and 2 were placed (at 16 and 11 cm from the heater). The relative humidity recorded by sensor 3, placed at 6 cm from the heater, increased sharply after a transitory drop and after 138 h it seems flooded. When the temperature of the heater was set to 140°C, the three sensors quickly recorded the corresponding increase of temperature, values of around 75°C being measured at 6 cm from the heater. Sensor 3, at 6 cm from the heater, recorded erratic values of relative humidity but with a trend to be lower than before (but always higher than 80 percent). Upon the increase of temperature of the heater, sensor 2 –at 11 cm from the heater– recorded a drop of relative humidity that was later recovered. Fluctuating values higher than 80 percent were subsequently recorded by sensor 2. Sensor 3 –at 16 cm from the heater– displayed relative humidity values fluctuating between 80 and 85 percent.

After 667 h of heating the hydration system was connected. This is considered as time 0 for the rest of the test. Figure 44 and Figure 45 show the evolution of temperature and relative humidity recorded by the sensors during the test. The two upper sensors measured temperatures around 40 and 55°C, reflecting the changes of the laboratory temperature. The sensor closest to the heater started to give negative or 0 values quite soon. The relative humidity values seem to correspond to sensors flooded (values higher than 100 percent). This is clear in sensor 1, whose transmission of the relative humidity failed very early. Sensor 3 provided erratic values of relative humidity due to the lack of temperature measurement, which the sensor needs to compute the relative humidity. The values given by this sensor are thus not reliable.

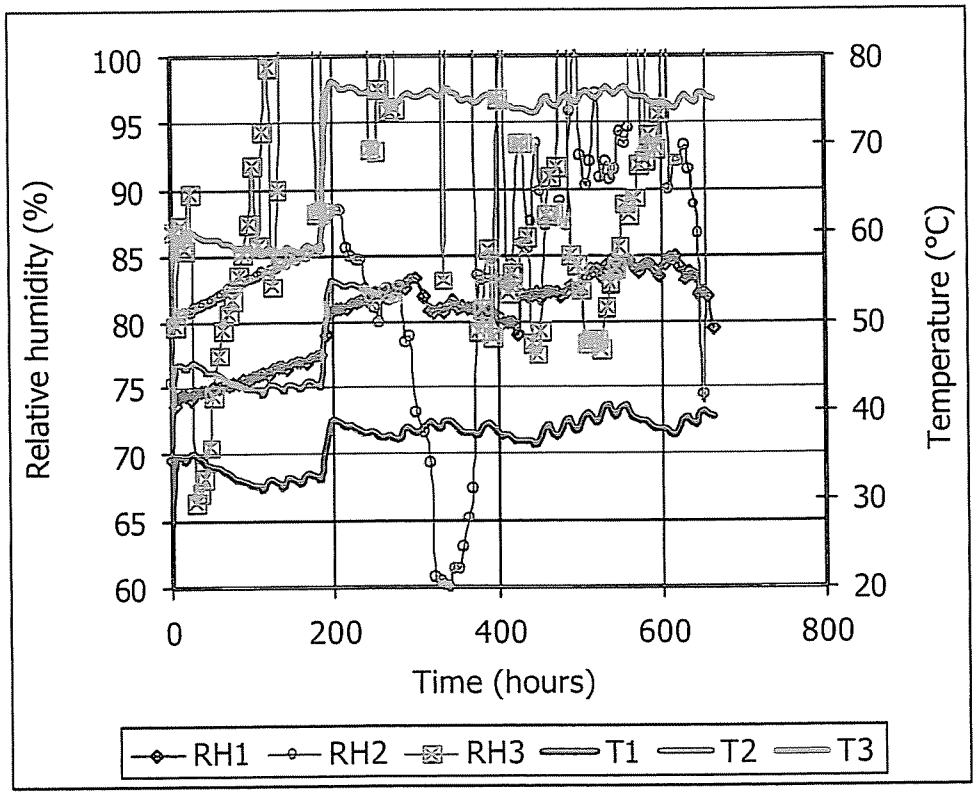


Figure 43: Evolution of relative humidity and temperature during the initial heating phase of test TBT20_2 (sensor 1 placed at 4 cm from the hydration surface, sensor 2 at 9 cm and sensor 3 at 14 cm)

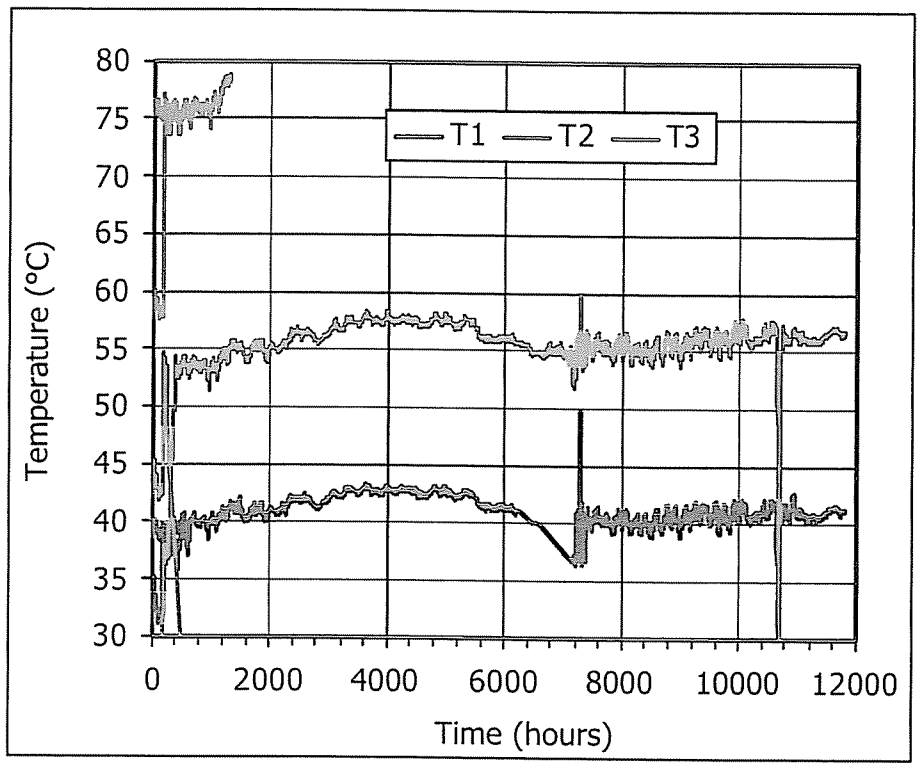


Figure 44: Evolution of temperature during the hydration/heating phase of test TBT20_2 (sensor 1 placed at 4 cm from the hydration surface, sensor 2 at 9 cm and sensor 3 at 14 cm)

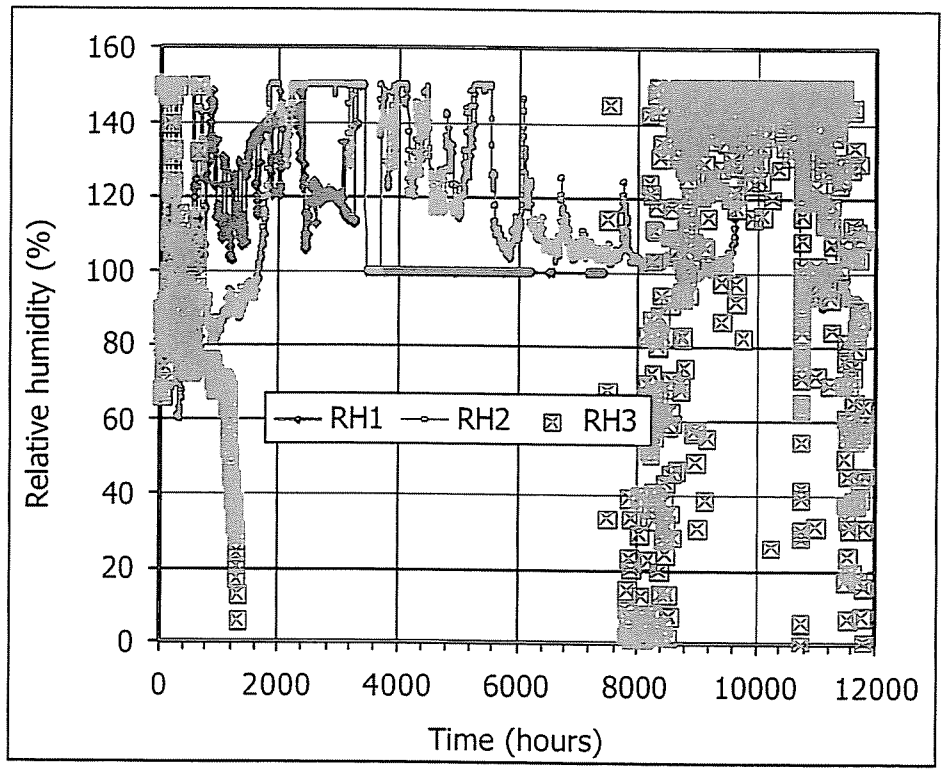


Figure 45: Evolution of relative humidity during the hydration/heating phase of test TBT20_2 (sensor 1 placed at 4 cm from the hydration surface, sensor 2 at 9 cm and sensor 3 at 14 cm)

At time 10643 h a blackout caused the heater, the cooling system in the upper part of the cell and the data acquisition to stop working. The power failure remained for four days and thus the whole system cooled to room temperature. Figure 46 shows the recovery of temperature and relative humidity when the heater and upper cooling were switched on again. It took 12 h to get the same temperatures in the bentonite as before the blackout. With respect to relative humidity, sensor 3 continued giving the non reliable, erratic values observed before; and sensor 2, that was recording values higher than 100 percent –attributed to flooding– started recoding values around 94 percent and remained so until the end of the tests. If water was condensed inside the sensor filter, cooling could have made it get out and allow the sensor to work properly afterwards.

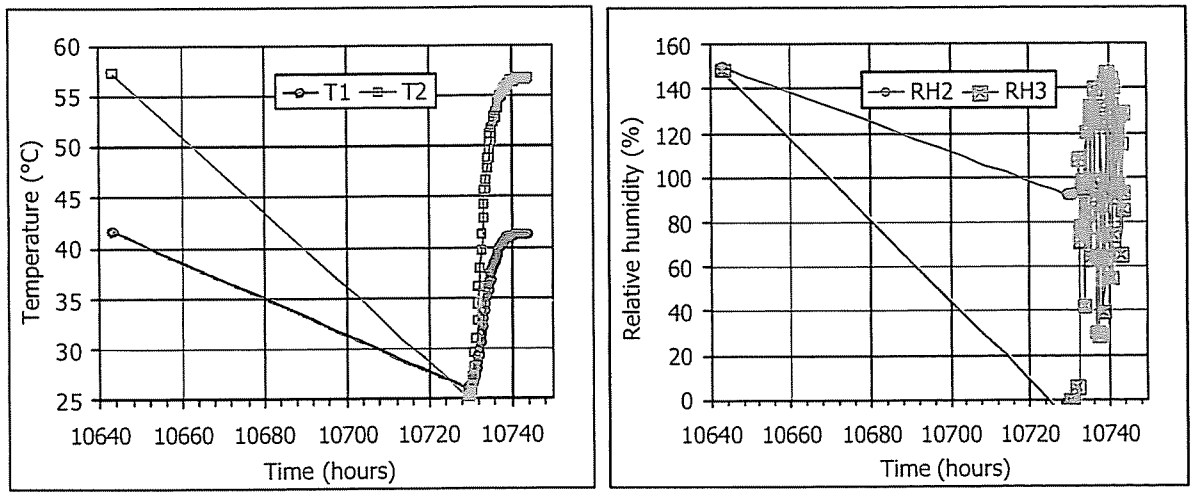


Figure 46: Recovery of temperature and relative humidity after the cooling caused by a power failure(sensor 1 placed at 4 cm from the hydration surface, sensor 2 at 9 cm and sensor 3 at 14 cm)

Figure 47 shows the water intake during hydration as measured by the volume change apparatus and by the balance (weight change). Despite the oscillations in weight, the trend of both curves was initially quite coherent. Towards time 5534 h, the hydration tube was accidentally disconnected from the cell, and the upper perforation for water intake remained open to atmosphere for 16 days. It is assumed that this fact did not yield a major lost of water through the upper perforation, since the temperature in the upper part of the bentonite is not high and the bentonite there is highly saturated. However, after reconnection of the hydration system, the water intake measured by the volume change apparatus changed its trend, displaying a sharp linear increase with a constant slope. This does not reflect any expected behaviour of bentonite hydration and in addition was not reflected in the weight changes. Therefore, this part of the water intake measurement performed by the volume change apparatus is considered faulty. With respect to the weight measurements, they present significant oscillations and are very much affected by temperature. Both facts make the weight measurement neither too reliable. The final trend of weight drop observed could be due to the spring-time increase of temperature in the laboratory.

Upon dismantling, it was checked by weight differences that the actual water intake had been of just 32 g. This corresponds approximately to the last weight recorded by the balance, 34 g.

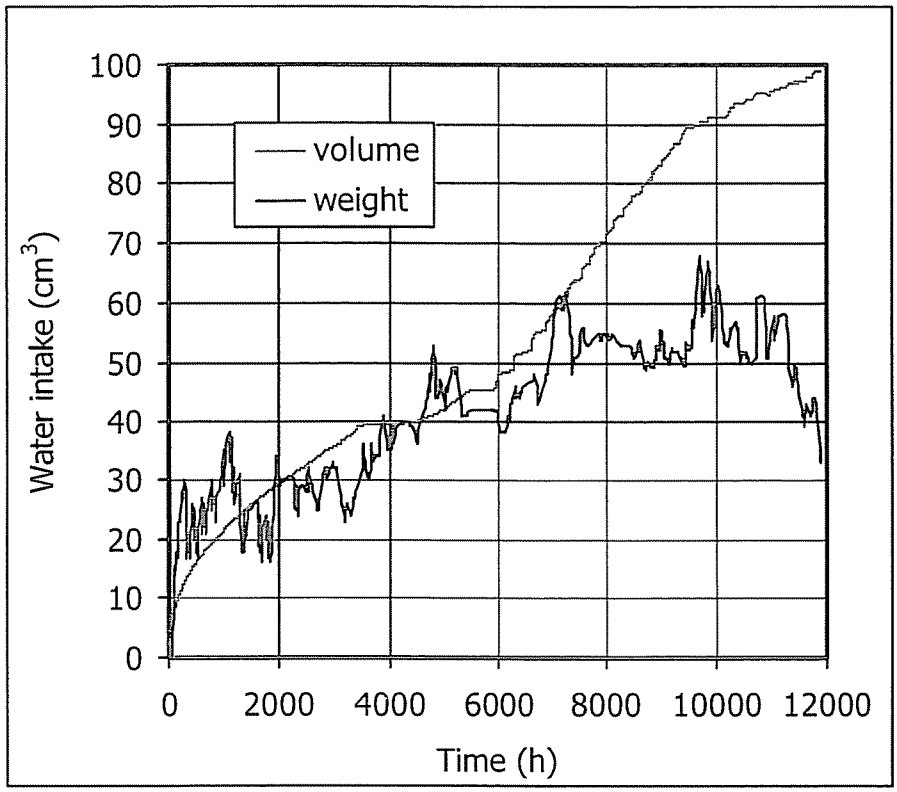


Figure 47: Water intake in test TBT20_2 as measured by the volume change apparatus and by the balance

The test was dismantled after 11903 hours (496 days) of operation (heating+hydration). The two blocks were not sealed between them. The height of the upper block had increased from 9.80 to 10.36 cm, whereas that of the lower block had decreased from 9.85 to 9.55 cm. The diameter in the upper part of the bentonite was of 7.17 cm and in the lower part, close to the heater, of 6.95 cm, the initial one being 7.02 cm. These changes in dimensions are a consequence of the swelling of the bentonite in the hydrated zones and of its shrinkage due to heating. The lower block developed vertical fissures upon extraction and cooling. The lower 2 cm of bentonite closest to the heater had turned black. In the upper block, near the stainless steel filter, an orange halo had developed in the lateral part of the block (Figure 48).

Figure 48: Appearance of the extracted lower (left) and upper (right) bentonite blocks of test TBT20_2

It was difficult to extract the sensors, specially the upper one, whose stainless steel filter broke during extraction. This is due to the huge swelling pressure developed by the saturated bentonite ($S_r$=94% in this area), since for a dry density of 1.56 g/cm$^3$, which is the one measured close to the sensor at the end of the test, the swelling pressure is higher than 7 MPa (Villar 2005). The lower sensor, placed at 6 cm from the heater, presented corrosion marks on its tip (Figure 49).

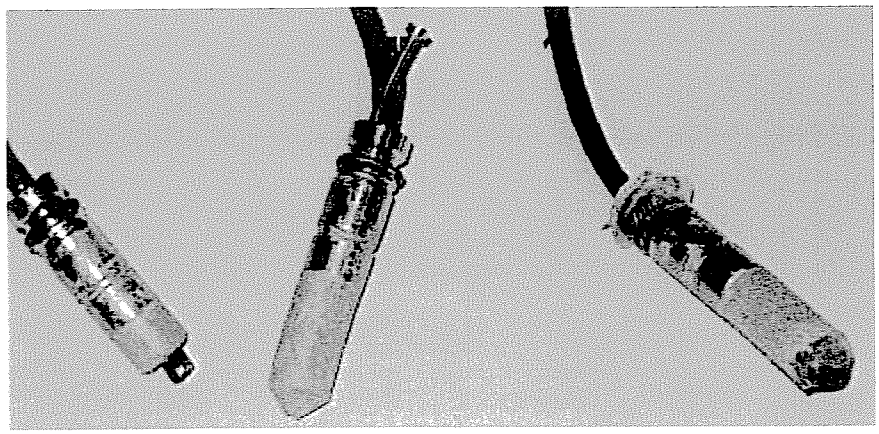

Figure 49: Final appearance of the sensors inserted in the bentonite in test TBT20_2 (left: upper sensor (broken during extraction), right: lower sensor with corrosion evidences)

The determination of water content along the bentonite reflected an intense drying, as can be seen in Table X and Figure 50. In fact, the final water content distribution was linear, from 31 percent near the hydration surface, to 0 percent near the heater, with an average value of 18 percent, which aggress with the final weight increase. The dry density along the bentonite changed accordingly, decreasing in the hydrated areas and increasing near the heater, as the dimensions of the blocks reported above confirm as well.

Table X: Final water content and dry density in test TBT20_2

| **Position* (cm)** | $w$ (%) | $\rho_d$ (g/cm$^3$) | $S_r$ (%) |
|---|---|---|---|
| 1 | 31.1 | 1.47 | 95 |
| 3 | 29.2 | 1.50 | 93 |
| 5 | 26.9 | 1.56 | 94 |
| 7 | 26.2 | 1.55 | 90 |
| 9 | 22.6 | 1.58 | 81 |
| 11 | 17.1 | 1.70 | 73 |
| 13 | 16.5 | 1.71 | 72 |
| 15 | 9.9 | 1.81 | 50 |
| 17 | 3.1 | 1.87 | 17 |
| 19 | 0.4 | 1.88 | 2 |
| Average | 18.3 | 1.66 | 67 |

*distance to hydration surface

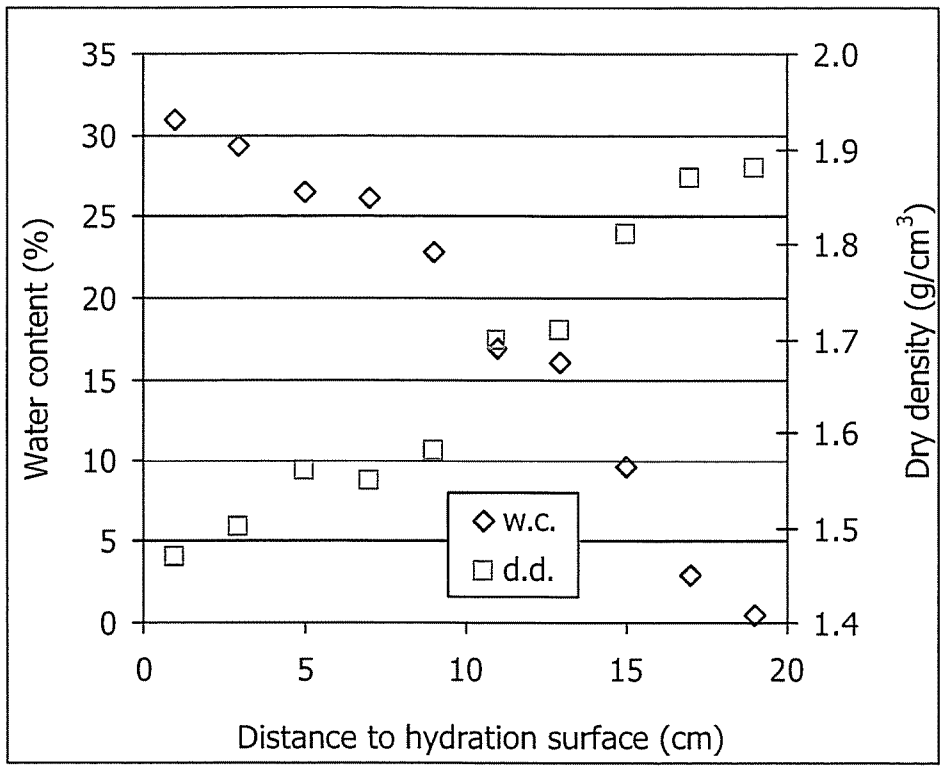


Figure 50: Final distribution of water content and dry density in test TBT20_2

### 4.6 Summary and discussion

Two hydration tests and three heating/hydration tests have been performed in blocks of compacted MX-80 bentonite, with measurements of water intake and, in some of them, temperature and relative humidity inside the clay. At the end of the tests the dry density and water content of the bentonite along the blocks have been determined.

The two hydration tests had similar duration but were performed in different 10-cm long cells. Despite the fact that test TBT10_2 presented an initial density gradient along the block (due to the manufacturing procedure) whereas the sample in test TBT10_3 was made of four small blocks piled up, the total water intake and final distribution of water content along the bentonite were analogous in both tests (Figure 51). This suggests that the results are reliable and also, on the one hand, that the influence of local density on the water uptake and distribution is negligible and, on the other, that the presence of discontinuities does not have a repercussion on water uptake and distribution. After one month the water content had increased even 10 cm away from the hydration surface.

The fact of working at high temperatures posed some experimental problems, particularly the preservation of the airtightness of the cells and the performance of the sensors. Thus, evaporation out of the cell could have taken place in the tests, what could have caused the clay desiccation near the heater area. The malfunctioning of the sensors could be caused by their being flooded by water condensed inside them.

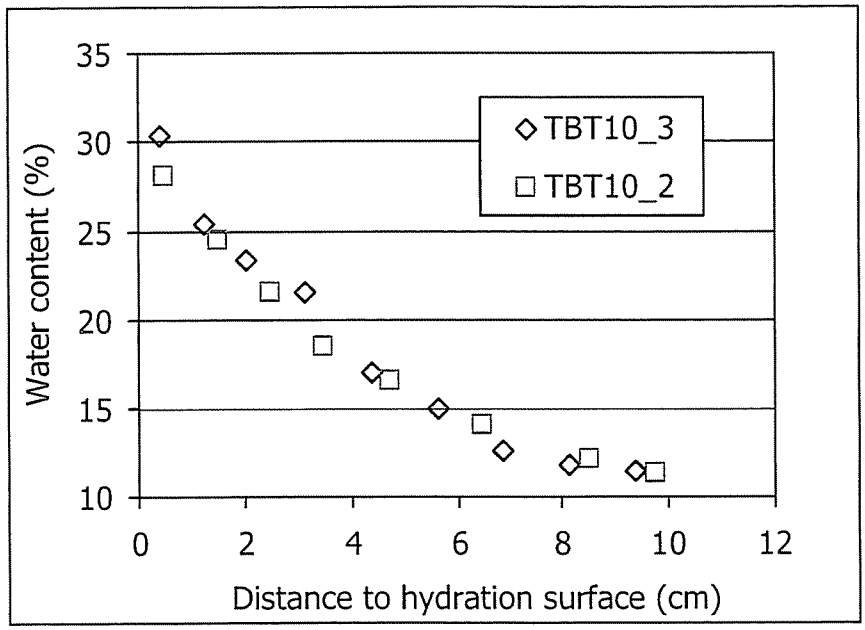


Figure 51: Final distribution of water content in two hydration tests performed on MX-80 bentonite compacted at nominal dry density 1.60 g/cm$^3$

The results of test TBT20_1 hint to a quick vapour generation and transfer upon heating (Figure 33), even though the bentonite was initially highly saturated (initial $S_r$ = 68 %). This fact could not be observed in test TBT20_2 because no data were recorded during the first hours. The temperatures inside the bentonite have barely changed during the tests, what points to small changes of the degree of saturation in each location during the experiments and consequently to a fast redistribution of water inside the clay that has persisted quite unchanged. Despite the fact that both tests are alike with respect to geometry and initial characteristics of the bentonite, the temperatures in test TBT20_2 are about 5°C lower than those recorded in the same positions in test TBT20_1 (compare Figure 34 and Figure 44). The differences between both tests are the starting-off procedure, that caused an important relative humidity gradient inside the clay before hydration started in test TBT20_2, the slightly higher water content of test TBT20_1 (16.7% *vs.* 15.8% for TBT20_2) and the use of a external stainless steel shell in test TBT20_1. The latter might be the reason of the higher temperatures recorded inside the clay, since the external steel shell promotes longitudinal heat transmission.

The total water intake in both tests was very low, 28 g in test TBT20_1, that lasted 337 days, and 32 g in test TBT20_2, that lasted 524 days. The online water intake measurement was not satisfactory in any of the tests, neither the relative humidity recordings of the sensors. The final water content and dry density along the bentonite in both tests are compared in Figure 52. The results are quite similar, the water content increasing in a linear way from almost 0 near the heater from values higher 30 percent near the hydration surface. The slightly higher water contents measured in test TBT20_1 in the upper part can be due to the higher initial water content of the bentonite (16.7 *vs.* 15.8%). Likewise, the dry density follows the same distribution pattern in both tests, although the values measured in test TBT20_2 are slightly higher, reflecting the higher initial dry density (1.70 *vs.* 1.67 g/cm$^3$). Thus the results of both tests are coherent. The extremely low average water content increase during the tests (2.2% in test TBT20_1 and 2.6% in test TBT20_2) can be attributed either to evaporation during the

test performance (which we have tried to avoid, specially in test TBT20_2) or to an actual behaviour of the bentonite, which could be unable to saturate under such high temperatures.

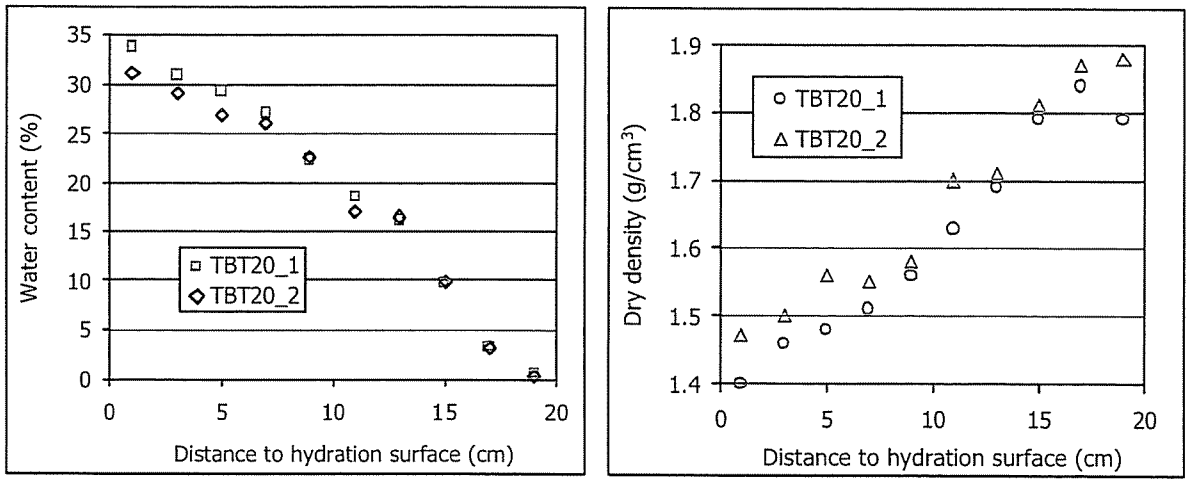


Figure 52: Final water content and dry density in two hydration+heating tests performed on MX-80 bentonite compacted at nominal dry density 1.70 g/cm$^3$ (test TBT20_1, 337 days, test TBT20_2, 524 days)

## 5. SUMMARY AND CONCLUSIONS

The results of the thermo-hydro-mechanical (THM) characterisation of the MX-80 bentonite performed by CIEMAT from 2004 to 2006 in the context of the Temperature Buffer Test have been presented. This characterisation has included the determination of the water retention curves of the bentonite at high temperature and the performance of infiltration tests under high thermal gradients.

To determine the retention curves a new methodology has been set up. It consists on the measurement of the relative humidity of blocks of bentonite compacted with different water contents while they are kept in a hermetic cell that can be heated on the outside. The results obtained agree with those obtained previously using other methodologies. They have shown the decrease of the retention capacity with temperature and the hysteresis between heating and cooling. In addition, the differences observed between the two densities tested (1.60 and 1.75 g/cm$^3$) become more important for the low suctions.

Two infiltration tests have been successfully carried out in bentonite compacted at nominal dry density 1.60 g/cm$^3$. After one month of hydration the water content increased all along the bentonite. This increase is not influenced by the existence of joints perpendicular to the flow and gives place to the swelling of the bentonite and to dry density changes.

The performance of infiltration tests under thermal gradient presented three major difficulties: the maintenance of the airtightness of the cell, the measurement of water intake and the proper functioning of the capacitive sensors, which became quickly flooded as a consequence of the intense water vapour generation. The vapour phase moves quickly even in the highly saturated material. The temperature gradient is established shortly after the initiation of the tests and remains constant for more than 10000 hours. The water intake of the

bentonite compacted at a nominal dry density of 1.70 g/cm$^3$ with an initial degree of saturation of 67-68 percent and saturated under a thermal gradient of 5.5 °C/cm (with a heater temperature of 140°C) is very low, even after more than 10000 hours. The distribution of water content and dry density along the bentonite follow a linear pattern, the dry density decreasing as the water content increases and increasing near the heater due to desiccation.

## 6. ACKNOWLEDGEMENTS

The research agreement CIEMAT/CIMNE 04/113 has financed this work. The collaboration of A. Ledesma (Technical University of Catalonia, Barcelona) and Manuel Velasco (DM-Iberia, Madrid) in the design of the infiltration tests is gratefully acknowledged. The laboratory work has been performed at the Soil Mechanics Laboratory of CIEMAT (Madrid, Spain) by R. Campos and J. Aroz. The software for the data acquisition of the tests has been developed by J.M. Barcala from CIEMAT.

## 7. REFERENCES

Hökmark, H. & Fälth, B. 2003. Temperature Buffer Test. Predictive Modelling Programme. Rev. 3. *SKB Äspö Hard Rock Laboratory* F12.1G. 1012125. Stockholm. 27 pp.

Madsen, F.T. 1998. Clay mineralogical investigations related to nuclear waste disposal. Clay Minerals 33: 109-129.

Müller-Vonmoss, M. & Kahr, G. 1983. Mineralogische Untersuchungen von Wyoming Bentonite MX-80 und Montigel. NTB 83-13. NAGRA, Wettingen. (In German).

Svensk Kärnbränslehantering AB. 2005. Äspö Hard Rock Laboratory. Annual Report 2004. SKB Technical Report TR-05-10. Stockholm. 211 pp.

Villar, M.V. 2002. Thermo-hydro-mechanical characterisation of a bentonite from Cabo de Gata. A study applied to the use of bentonite as sealing material in high level radioactive waste repositories. Publicación Técnica ENRESA 01/2002. 258 pp. Madrid.

Villar, M.V. 2005. MX-80 bentonite. Termo-hydro-mechanical characterisation performed at CIEMAT in the context of the Prototype Project. Informes Técnicos CIEMAT 1053. 39 pp. Madrid.

Villar, M.V. & Lloret, A. 2004. Influence of temperature on the hydro-mechanical behaviour of a compacted bentonite. Applied Clay Science 26: 337-350.

Villar, M.V., Martín, P.L. & Lloret, A. 2005a. Determination of water retention curves of two bentonites at high temperature. In: Tarantino, A., Romero, E. & Cui, Y.J. (eds.): Advanced experimental unsaturated soil mechanics. EXPERUS 2005. A.A. Balkema Publishers. London, pp 77-82.

Villar, M.V., P.L. Martín & J.M. Barcala. 2005b. Infiltration tests at isothermal conditions and under thermal gradient. Technical Report CIEMAT/DMA/M2140/1/05. 25 pp. Madrid.